ANKARA UNIVERSITY FACULTY OF PHARMACY

ISOPS 13th International SYMPOSIUM ON PHARMACEUTICAL SCIENCES

Poster no	Presenter	Title	Topic
A31	H. Kerem Polat	INCREASING RIBOFLAVIN SOLUBILITY WITH SULFOBUTYL ETHER-B-CYCLODEXTRIN AND FORMATION OF DRUG- CYCLODEXTRIN INCLUSION COMPLEXES	Pharmaceutical Technology
A32	Yasin Turanlı	BUDESONIDE LOADED CONTROLLED-RELEASE POLYCAPROLACTONE NANOPARTICLES	Pharmaceutical Technology
A33	Zeliha Duygu Özdal	EFFECT OF POLYMER ON ONDANSETRON HCl LOADED POLYMERİC NANOPARTİCLES	Pharmaceutical Technology
A34	Tuba İnceçayır	IN SILICO PREDICTION OF INTESTINAL DISSOLUTION AND ABSORPTION OF CARBAMAZEPINE IN HUMANS	Pharmaceutical Technology
A35	Tuba İnceçayır	EVALUATION OF A BIPHASIC IN VITRO DISSOLUTION TEST FOR LAMOTRIGINE IMMEDIATE RELEASE TABLETS AND CORRELATION TO HUMAN IN VIVO PERFORMANCE	Pharmaceutical Technology
A36	Şeyma Adatepe	PREPARATION AND EVALUATION OF ALPHA TOCOPHEROL/CYCLODEXTRIN COMPLEXES	Pharmaceutical Technology
A37	Ulya Badıllı	SEMISOLID NLC FORMULATIONS FOR COSMETIC USE: EVALUATION OF MECHANICAL PROPERTIES	Pharmaceutical Technology
A38	Özge Eşim	PREPARATION AND IN VITRO CHARACTERIZATION OF LIPID-COATED NANOPARTICLES CONTAINING CARBOPLATIN AND DECITABINE	Pharmaceutical Technology
A39	Özlem Çulcu	DEVELOPMENT AND CHARACTERIZATION OF BUCCAL FILM CONTAINING HYDROCORTISONE NANOSUSPENSIONS	Pharmaceutical Technology
A40	Burcu Devrim	PREPARATION AND EVALUATION OF LYSOZYME LOADED POLYCAPROLACTONE MICROPARTICLES USING THE FULL FACTORIAL DESIGN	Pharmaceutical Technology
A41	Emrah Akgeyik	INVESTIGATION OF MISCELLISATION CHARACTERISTICS OF POLYOXYL CASTOR OIL FOR VITAMIN D3 PREPARATIONS IN TURKISH DRUG MARKET	Pharmaceutical Technology
A42	Kadir Aykaç	LACOSAMIDE LOADED MICRONEEDLES AS NASAL DRUG DELIVERY SYSTEMS	Pharmaceutical Technology
A43	Seval Olgaç	MODELING AND COMPARISON OF IN VITRO DISSOLUTION PROFILES OF NAPROXEN SODIUM TABLETS IN BIORELEVANT MEDIA	Pharmaceutical Technology
A44	Seval Olgaç	VALIDATED HPLC METHOD FOR THE DETERMINATION OF TENOFOVIR AND ITS APPLICATION FOR IN-VITRO AND EX-VIVO INVESTIGATIONS OF TENOFOVIR LOADED DOUBLE NANOEMULSION	Pharmaceutical Technology
A45	Fetza Şebnem Görür	INTRANSAL DELIVERY OF NIOSOMAL MELATONIN FOR ALZHEIMER'S DISEASE	Pharmaceutical Technology
M1	Tugba Gencoglu	SYNTHESİS OF CİSPLATİN AND/OR GEMCİTABİNE CONTAİNİNG POLYMERİC NANODRUG FORMULATİONS FOR BREAST CANCER TREATMENT	Biotechnology
M2	Ümmügülsüm Tanman	TRANSCRIPTOMIC CHARACTERIZATION OF THE USNIC ACID (UA) EFFECTS ON TRIPLE NEGATIVE BREAST CANCER (TNBC) WITH NEXT GENERATION SEQUENCING TECHNOLOGY	Biotechnology
M3	Ümmügülsüm Tanman	DETERMINATION THE USNIC ACID (UA) THERAPY EFFECTS ON TRIPLE NEGATIVE BREAST CANCER (TNBC) BY PROTEOMIC APPROACHES	Biotechnology
M4	Gülşah Yiğit Erdem	INVESTIGATION OF THE EFFECTIVENESS OF GLYCOPOLYMER BASED THERANOSTIC NANOSISTEMS IN BREAST CANCER	Biotechnology
M5	Gözde Ultav	DETERMİNATİON OF EFFECTİVE SURFACE MODİFİCATİONS OF SİLİCA NANOPARTİCLES AS VEGF-TARGETED SİRNA CARRİERS	Biotechnology

INCREASING RIBOFLAVIN SOLUBILITY WITH SULFOBUTYL ETHER-B-CYCLODEXTRIN AND FORMATION OF DRUG- CYCLODEXTRIN INCLUSION COMPLEXES

[1]Polat H. K., [2]Aytekin E, [2]Kurt N., [2] Bozdag Pehlivan S, [2] Çalış S

[1]Erzincan Binali Yıldırım University, Faculty of Pharmacy, Department of Pharmaceutical Technology, Erzincan

[2] Hacettepe University, Faculty of Pharmacy, Department of Pharmaceutical Technology, Ankara

INTRODUCTION

Keratoconus is a degenerative disease that causes cone-shaped swelling of the cornea and causes thinning in advanced stages. Since riboflavin is susceptible to light, it has been used to initiate ultraviolet-induced collagen cross-linking in the diseased cornea since 2003 (1). The commonly used method to facilitate riboflavin-mediated corneal cross-linking is an invasive technique with removing the epithelium performed under local anesthesia. It is essential to develop formulations that can increase riboflavin penetration due to increased riboflavin solubility without removing the epithelium surgically. In this study, we investigated the effects of Sulfobutyl ether-β-cyclodextrin (SBE-β-CD) on riboflavin solubility and whether the drug-cyclodextrin inclusion complex was successfully produced.

MATERIALS AND METHODS

Phase-solubility studies were carried out using Loftson and Brewster methods (2). Briefly, abundant riboflavin was added to SBE-β-CD solutions with increasing concentrations (0–10 mM), and the mixtures were stirred at room temperature for seven days with a magnetic stirrer. Later, each mixture was filtered through a 0.22 µm membrane filter, and the riboflavin amount in the supernatant was determined by HPLC (Table I). The riboflavin inclusion complexes: SBE-β-CD; were prepared by kneading methods. Fourier transform infrared spectroscopy (FTIR-ATR), and Differential scanning calorimetry (DSC) analyzes were conducted to determine the successful formation of drug-CD inclusion complexes.

Table 1: HPLC conditions

Mobile Phase	Acetate Buffer (Sodium acetate/CaCl2/EDTA):Methanol
Injection Volume	200 µL
Flow rate	1 mL.min^{-1}
Detector Wavelength	Fluorescent (Excitation: 420 nm / Emission: 530 nm)
Column	C8 Column
Column Temp.	23 ℃

RESULTS

According to the defined methodology, the diagram of SBE-β-CD was classified as "AL-type''. From the straight lines of SBE-β-CD (r2 = 0,9765). The determined slopes were 0,0135. The complexation efficiency (EC) was 0,013 and the stability constant (KS) 62 M^{-1} (Figure 1).

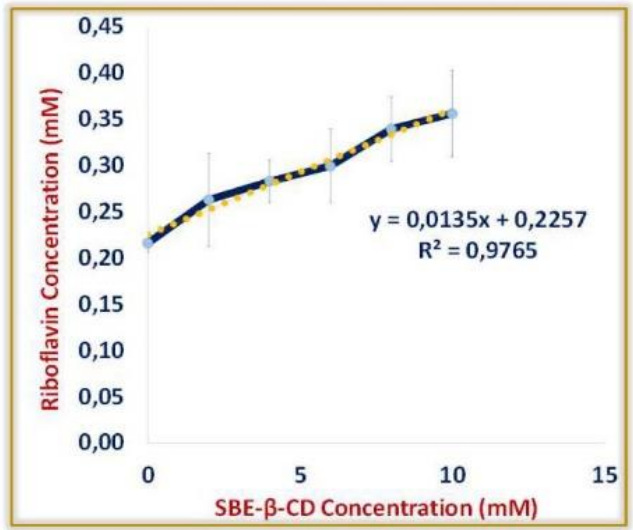

Figure 1: Phase solubility diagrams

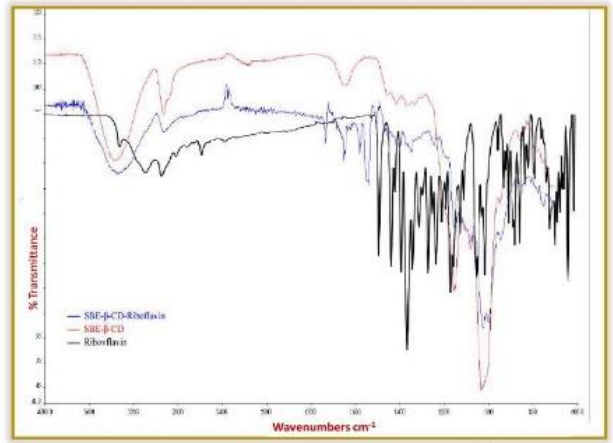

Figure 2:FTIR spectra of Riboflavin, SBE-β-CD-, SBE-β-CD-Riboflavin complex

When FTIR results were evaluated for confirming SBE-β-CD-Riboflavin complex, specific peaks of riboflavin were observed for pure drug and these peaks disappeared in the complex prepared by kneading (Figure 2).

When DSC thermograms of riboflavin, It was observed that a peak for riboflavin at 304 °C (melting point) was absent. Also, the melting peak of riboflavin are disappeared in the SBE-β-CD-Riboflavin complex (Figure 3).

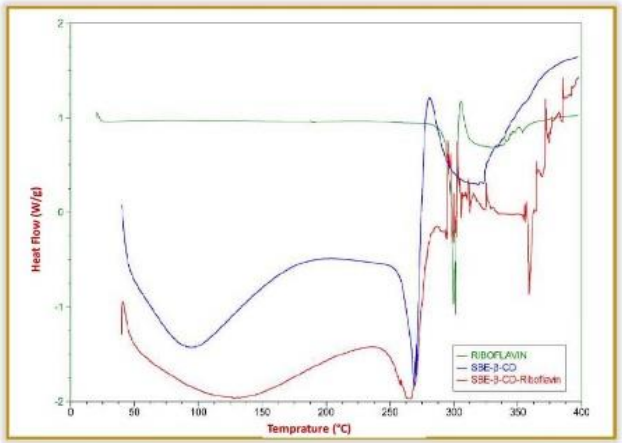

Figure 3:DSC thermogram of Riboflavin, SBE-β-CD-, SBE-β-CD-Riboflavin complex

Conclusions

This study has demostrated the the solubility of riboflavin could be enhanced using SBE-β-CD. Further studies will be conducted to investigate whether increasing the solubility of riboflavin by complexing with SBE-β-CD enhances corneal permeation of the drug ex-vivo and in vivo.

References:

1.Aytekin E, Öztürk N, Vural İ, Polat HK, Çakmak HB, Çalış S, Pehlivan SB. J Control Release. 2020;324:238-249.

2. Loftsson T, Brewster ME.. J Pharm Pharmacol. 2010 ;62(11):1607-21.

JUNE 22-25, 2021 ANKARA, TURKEY
13th International Symposium on Pharmaceutical Sciences

BUDESONIDE LOADED CONTROLLED-RELEASE POLYCAPROLACTONE NANOPARTICLES

Yasin Turanlı, Füsun Acartürk
Gazi University, Faculty of Pharmacy, Department of Pharmaceutical Technology, Turkey
yasin.turanli@gmail.com

13th International Symposium on Pharmaceutical Sciences
JUNE 22-25, 2021
ANKARA, TURKEY

Introduction

- Corticosteroids such as budesonide are the drugs of choice for the treatment of inflammatory disorders[1].
- However, budesonide undergoes extensive hepatic first-pass metabolism to the extent of approximately 85%.
- This imposes the need for either frequent administration of this drug or high doses[1].

Aim

To overcome first-pass metabolism and attain controlled release, budesonide was encapsulated in a biodegradable polymer, polycaprolactone (PCL).

Materials and Methods

- Budesonide-loaded PCL (MW 80,000) nanoparticles were prepared by emulsion solvent evaporation with ultrasonification technique (Fig 1).
- Formulations were prepared based on 3^2 factorial design (Table 1).
- Independent variables were the concentration of polymer and oil phase:aqueous phase ratio.
- Particle size, polidispersity index and zeta potential were determined using Malvern Zetasizer Nano ZS (Table 2-3).

Table 1. Independent variables and their levels in the experimental design

Independent variables		Levels		
		-1	0	+1
PCL concentration (%)		1	2	3
Organic phase/Aqueous phase		1:8	1:9	1:10
Dependent variables	Desired Outcomes			
Particles size (nm)	Minimize			
Polidispersity index	Minimize			
Zeta potential (mV)	Maximize			

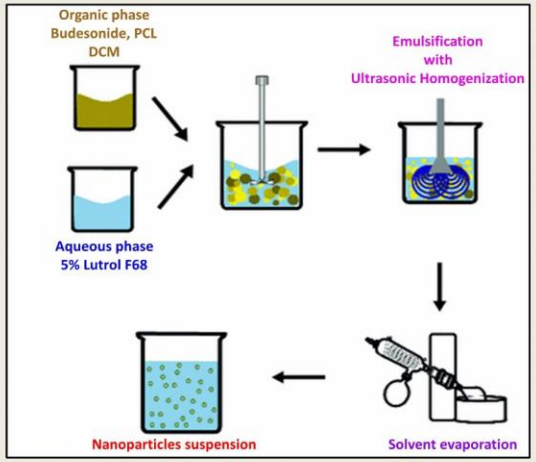

Figure 1. Schematic illustration of nanoparticles preparation

Results

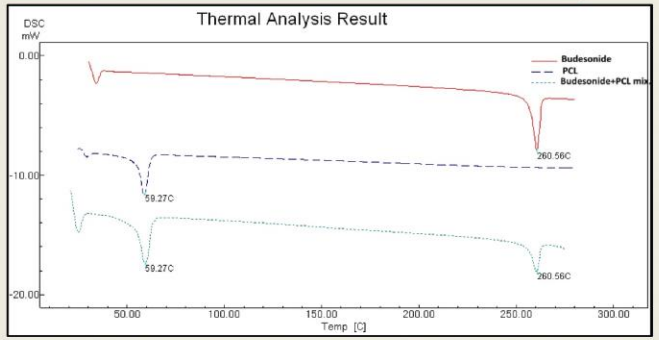

Figure 2. DSC thermograms of budesonide, PCL, and drug-polymer mixture

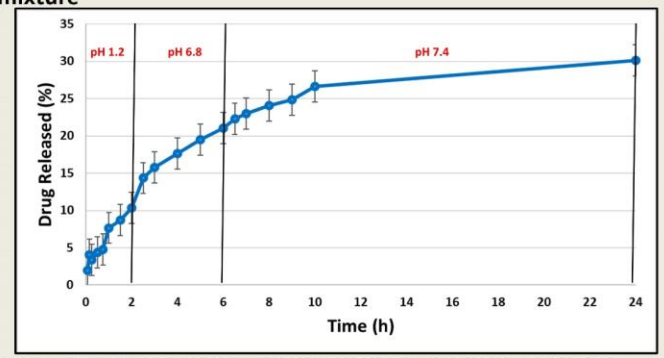

Figure 3. Release profile of budesonide loaded nanoparticles

Table 2. Physical properties of PCL nanoparticles

Formulation	PCL %	LUTROL F68 %	Organic phase/Aqueous phase	Mean particle dimeter	PDI	Zeta potential
NP1	1	5	1:8	214,5	0,242	-23,0
NP2	1	5	1:9	205,5	0,239	-13,3
NP3	1	5	1:10	249,1	0,283	-17,0
NP4	2	5	1:8	315,1	0,424	-15,7
NP5	2	5	1:9	374,5	0,577	-18,4
NP6	2	5	1:10	385,2	0,314	-21,8
NP7	3	5	1:8	1059,5	0,942	-10,8
NP8	3	5	1:9	389,9	0,564	-10,9
NP9	3	5	1:10	433,5	0,141	-11,2

Table 3. Physical properties of budesonide loaded nanoparticles

Formulation	BUD %	PCL %	LUTROL F68 %	Organic phase/Aqueous phase	Mean particle diameter	PDI	Zeta potential
NP1 (1)	0,5	1	5	1:8	220,4	0,167	-19,9
NP1 (2)	1	1	5	1:8	245,1	0,221	-20,4
NP1 (3)	2	1	5	1:8	215,4	0,223	-14,5

- ✓Thermal studies confirmed that there was no interaction between drug and polymer.
- ✓Among the formulations prepared according to the factorial design, the NP1 formulation was determined as the optimum formulation due to its high zeta potential and low particle size.
- ✓Budesonide loaded NP1 formulation was prepared at 3 different concentrations.
- ✓NP1(2) formulation was determined as the appropriate formulation due to its high zeta potential and an in vitro release study was performed. Nanoparticle formulations had high encapsulation efficiencies (84,2±2,4 %)
- ✓As a result of in vitro drug release studies, approximately 35% of the active substance released from the particles. The hydrophobic character of budesonide resulted in a low release rate.

Conclusions

- ✓Budesonide loaded PCL nanoparticles were successfully prepared. However, the active substance released slowly from the particles.
- ✓Therefore, either a PCL polymer with a lower molecular weight should be used or particles with a higher drug/polymer ratio can be prepared with a different method and the release can be completed within 24 hours.

Acknowlegments

This study was supported by Gazi University Scientific Research Projects Coordination Unit under grant number 02/2019-14. Eudragit polymers were generously supplied by Evonik Chemicals and budesonide by Deva Pharmaceuticals, Istanbul, Turkey.

References

Midhun, B. T., Shalumon, K. T., Manzoor, K., Jayakumar, R., Nair, S. V., & Deepthy, M. (2011). Preparation of budesonide-loaded polycaprolactone nanobeads by electrospraying for controlled drug release. *Journal of Biomaterials Science, Polymer Edition*, *22*(18), 2431-2444.

EFFECT OF POLYMER ON ONDANSETRON HCl LOADED POLYMERIC NANOPARTICLES

[1,2]Ozdal Z.D., [1]Takka S.

[1] Gazi University, Faculty of Pharmacy, Department of Pharmaceutical Technology, Ankara, Turkey, z.duygu.ozdal@gmail.com,
[2]Erzincan Binali Yıldırım University, Faculty of Pharmacy, Department of Pharmaceutical Pharmaceutical Technology, Erzincan, Turkey

JUNE 22-25, 2021 ANKARA, TURKEY
13th ISOPS International SYMPOSIUM ON PHARMACEUTICAL SCIENCES
ANKARA UNIVERSITY FACULTY OF PHARMACY

Introduction

Ondansetron HCl (OND) is an antagonist of serotonin (5-hydroxytryptamine) subtype 3 receptor which is used preventing and treatment of nausea and vomiting in neoplastic patients [1]. Its absorbed fastly but has a half-life between 2-4 hours that is relatively short [2, 3]. In this situation, it required administration frequently.

This study aimed to investigate the effect of amount and copolymer composition on OND-loaded nanoparticles (NPs).

Table 1. Composition of Nanoparticles

			FORMULATION CODE					
			NP1	NP2	NP3	NP4	NP5	NP6
ORGANIC PHASE	POLYMER	PLGA(50:50) 7-17 kDa	240 mg	320 mg	400 mg			
		PLGA (50:50) 38-54 kDa				400 mg		
		PLGA (65:35) 24-38 kDa					400 mg	
		PLGA (75:25) 4-15 kDa						400 mg
	ORGANIC SOLVENT	DCM	4ml	4ml	4ml	4ml	4ml	4ml
INNER AQUEOUS PHASE	ACTIVE INGREDIENT	ONDANSETRON HCl	4mg	4mg	4mg	4mg	4mg	4mg
	SURFACTANT	PVA 31-50	1.6 ml	1.6 ml	1.6 ml	1.6 ml	1.6ml	1.6 ml
EXTERNAL AQUEOUS PHASE	SURFACTANT	PVA 31-50	6 ml	6 ml	6 ml	6 ml	6 ml	6 ml

Methods

Preparation of OND Loaded Nanoparticles

OND loaded NPs were prepared by the modified double emulsion solvent evaporation method. The composition of NPs are presented in Table 1.

Characterization of Nanoparticles

Particle Size and Zeta Potential
The particle size, polydispersity index (PDI) and zeta potential were measured using a Malvern Zeta Sizer (Nano ZS)

Encapsulation Efficiency (EE%)
The amount of OND was analyzed by HPLC after lyophilized NPs were distrupted with acetonitrile.

In Vitro Drug Release

Franz diffusion technique

Results

Table 2. Characterization of Nanoparticles

Formulation Code	Particle Size (nm)	PDI	Zeta Potential (mV)	EE (%)
NP1	373.2 ± 12.55	0.336 ± 0,02	-17.40 ± 0.80	25.85 ± 0.72
NP2	332.6 ± 2.59	0.297 ± 0.05	-19.53 ± 0.68	37.5 ± 2.68
NP3	318.9 ± 15.11	0.346 ± 0.02	-11.50 ± 1.31	39.48 ± 5.78
NP4	404.9 ± 4.37	0.146 ± 0.07	-8.82± 0.33	20.66 ± 2.15
NP5	396.2 ± 0.39	0.280 ± 0.03	-14.70 ± 0.17	25.78 ± 1.02
NP6	366.0 ± 7.09	0.272 ± 0.04	-17.73 ± 0.75	35.54 ± 2.02

A)

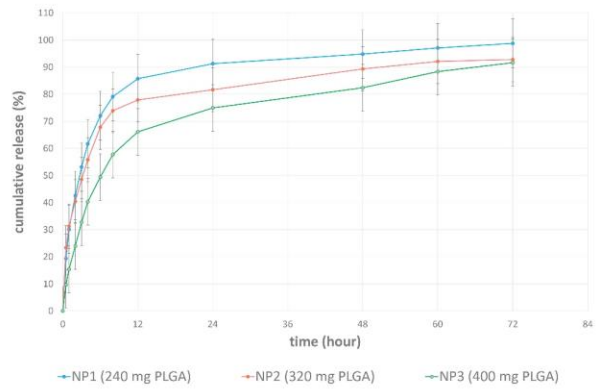

B)

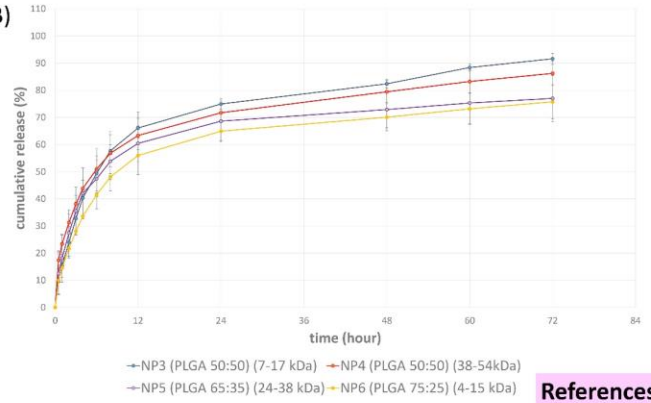

Figure 1. Release profile of OND loaded NPs. A) Effect of amount of polymer and B) Effect of compositionand molecular weight of polymer

Discussion:

The result of this investigation showed that the molecular weight, amount and copolymer composition of PLGA cause different characterization.

It was found that EE% of the NP3 formulation, which used a higher amount of polymer, was higher than NP1 and NP2.

It was observed that the EE% of NP3 formulation using polymer with a lower molecular weight was higher than that of NP4.

The increase in the lactic acid ratio in the PLGA copolymer causes an increase in lipophilicity and, therefore a decrease in the degradation rate.

Hence the NP6 formulation showed the lowest release rate at the end of 72 h.

References:

1. Duong, V. A., et al.,(2019). Journal of Drug Delivery Science and Technology, 53, 101185.
2. Sonje, A. G., & Mahajan, H. S. (2016). Materials Science and Engineering: C, 64, 329-335.
3. Ye, J. H., et al.,(2001). CNS drug reviews, 7(2), 199-213.

IN SILICO PREDICTION OF INTESTINAL DISSOLUTION AND ABSORPTION OF CARBAMAZEPINE IN HUMANS

Department of Pharmaceutical Technology, Faculty of Pharmacy, Gazi University, 06330 Ankara, Turkey
Tuba Incecayir, Sedef Benli
Correspondence: tincecayir@gazi.edu.tr

INTRODUCTION

The aim of this study was to predict the intestinal dissolution and absorption of carbamazepine (CBZ) in humans using gastrointestinal simulation technology.

MATERIALS AND METHODS

- Gastrointestinal simulation based on the advanced compartmental absorption and transit model (GastroPlus version 9.6, SimulationsPlus, Lancaster, CA) was used for the prediction.
- The plasma concentration-time profiles of 200 mg CBZ IR tablet were simulated based on the physicochemical and pharmacokinetic (PK) properties of the drug (Table 1, Fig.1.).
- The simulation was performed for 72 h using population simulation mode.
- The amounts of drug dissolved and absorbed as a fuction of time and regional absorption were predicted for human fasted and fed states.

Table 1. The physicochemical and pharmacokinetic input parameters of carbamazpine (1-3)

MW	238.29
Solubility (at pH 6.5) (C_s) (mg/mL)	0.117
log P	1.65
pK_a	11.83
Human jejunal permeability (P_{eff}) (cm/s)	4.3 x 10^{-4}
Unbound percent in plasma (f_u) (%)	30
Clearance (L/h)	4.91
Volume of distribution (V_c) (L/kg)	1.26
Dose volume (mL)	250
Mean precipitation time (sec)*	900
Drug particle density (g/mL) *	1.2
Effective particle radius (µm) *	25

*default values

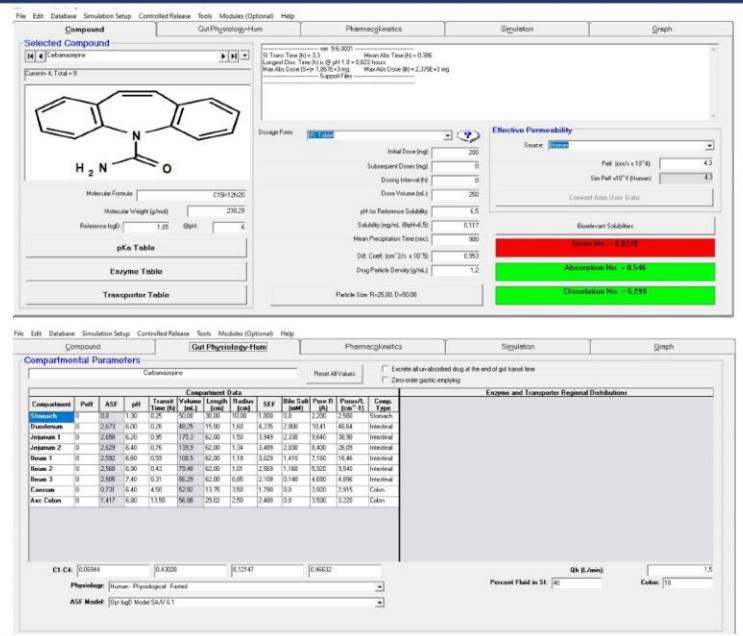

Figure 1. Compound and human gut physiology tabs of the program.

RESULTS and DISCUSSION

The simulated plasma profiles of 200 mg CBZ IR tablet are presented in Fig.2.

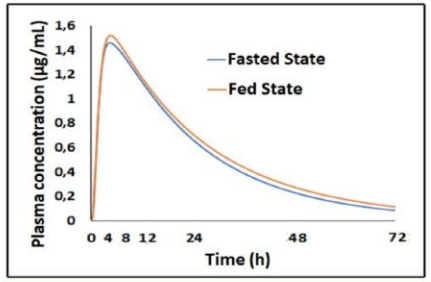

Figure 2. Simulated plasma profiles for 200 mg CBZ IR tablet.

RESULTS and DISCUSSION

- The predicted AUC_{0-72}, and C_{max} were 38.2 vs. 41.1 µg/mL.h and 1.47 vs. 1.54 ug/mL in fasted and fed states, respectively. t_{max} (4.5 h) was not changed in fasted and fed states.
- The regional absorption and profiles of drug dissolved in vivo are presented in Fig. 3.

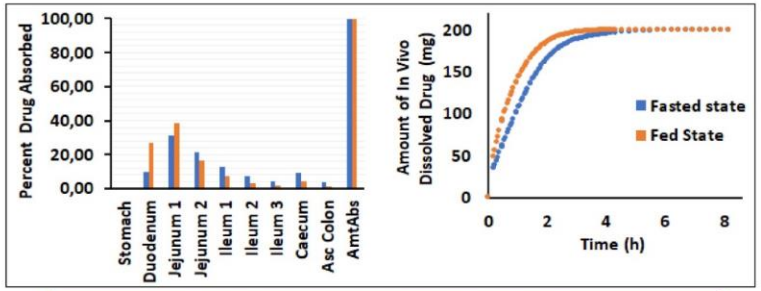

Figure 3. Regional absorption and in vivo dissolved amounts of CBZ from 200 mg IR tablet in fasted and fed states.

CONCLUSION

The in silico prediction of intestinal dissolution and absorption of CBZ indicated that food intake seems not to effect the oral bioavailability of CBZ IR tablets significantly.

REFERENCES

1.Kovacevic I. et al. (2009) Molecular Pharmaceutics, 6 (1):40-7.
2.Djordjevic N. et al (2017) European Journal of Drug Metabolism and Pharmacokinetics, 42:729-44.
3.Hemenway J. et al. (2007) Bioorganic and Medicinal Chemistry Letters, 17: 6629-32.

ACKNOWLEDGEMENTS

The authors declare no conflicts of interest.

EVALUATION OF A BIPHASIC IN VITRO DISSOLUTION TEST FOR LAMOTRIGINE IMMEDIATE RELEASE TABLETS AND CORRELATION TO HUMAN IN VIVO PERFORMANCE

Department of Pharmaceutical Technology, Faculty of Pharmacy, Gazi University, 06330 Ankara, Turkey
Tuba Incecayir, M. Enes Demir
Correspondence: tincecayir@gazi.edu.tr

INTRODUCTION

The aim of this study was to characterize the dissolution profiles of two IR tablets of lamotrigine (LTG) with the biphasic dissolution test and explore the correlation to in vivo.

MATERIALS AND METHODS

MATERIALS

- LTG (Fig. 1) was kindly supplied from Sanovel Pharmaceuticals (Istanbul, Turkey).
- 1-octanol, KH_2PO_4 and NaOH were purchased from Sigma-Aldrich (Germany).
- IR tablet formulations of 200 mg LTG (Reference, batch no: A8158013 and Test, batch no: 19143001) purchased from the local drug market were tested.

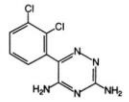

Figure 1. Chemical structure of lamotrigine

Physicochemical Properties	
MW	256.1
pKa	5.7
logP oct	2.5

METHODS

Biphasic Dissolution Test

- Biphasic test was performed using USP apparatus II (708-DS, Agilent Technologies) with the modification illustrated in Fig. 2 (37 ºC, 50 rpm).
- pH 6.8 phosphate buffer and octanol were used as the aqueous and organic phases, respectively (300:200 (mL:mL, aqueous:organic)).
- Samples were withdrawn at predetermined time points, and filtered using a 0.45 µm syringe filter. Aqueous and organic samples were analyzed spectrophotometrically at 305 and 310 nm, respectively.

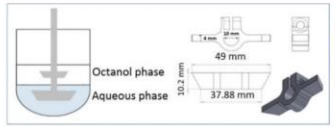

Figure 2. Schematic depiction of biphasic dissolution system and the additional pallet

Data Analysis

- f_2 similarity test was used to compare dissolution profiles.

$$f_2 = 50 \log \frac{100}{\sqrt{1+\frac{1}{n}\sum_{t=1}^{n}(R_t - T_t)^2}} \quad Eq.(1)$$

R_t and T_t : cumulative percentage dissolved at time point t for the reference and test products
n: number of sampling points

METHODS

Data Analysis

- The pharmacokinetic data were derived from the published paper to assess in vivo relevance (1).
- Wagner−Nelson method (Eq. 2) was used to calculate the fraction of LTG absorbed (F_{abs}) from the plasma data of reference (1, 2).

$$F_{abs} = \frac{k_e \int_0^t C(t)dt + C(t)}{k_e \int_0^\infty C(t)dt} \quad Eq.(2)$$

C(t): drug concentration in plasma
k_e : elimination rate constant

- F_{abs} was correlated to the fraction of LTG partitioned in octanol (F_{diss})
- The correlation was used to predict F_{abs} and plasma profiles of the test product.

RESULTS and DISCUSSION

- Dissolution profiles of LTG determined from two phases for test and reference products are presented in Fig. 3.
- Test product exhibited dissolution profile similarity to reference product ($f_2 > 50$).
- The calculated F_{abs} vs. partitioned LTG in octanol is presented in Fig. 4.

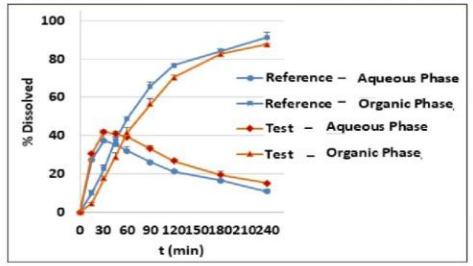

Figure 3. Dissolution profiles of test and reference products in the aqueous and octanol phases of the biphasic system.

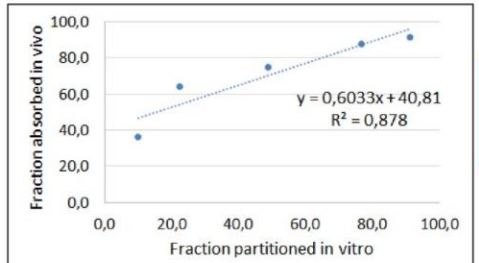

Figure 4. Correlation between the calculated F_{abs} and the fraction of LTG partitioned in the organic phase.

RESULTS and DISCUSSION

- Mean plasma concentration-time profiles of LTG from reference (observed) and test (predicted) are presented in Fig.5.
- AUC, C_{max} and t_{max} values were 122±28 vs.119±25 ug/mL.h, 2.9±0.5 vs. 2.6±0.4 ug/mL and 2.5±1.2 vs. 3.7±1.1 h for the reference and test, respectively.
- The bioequivalence (BE) of the test vs. reference was 83.1-111% for AUC and 80.2-100% for C_{max} with a 90% CI, which falls within the 80-125% BE criteria.

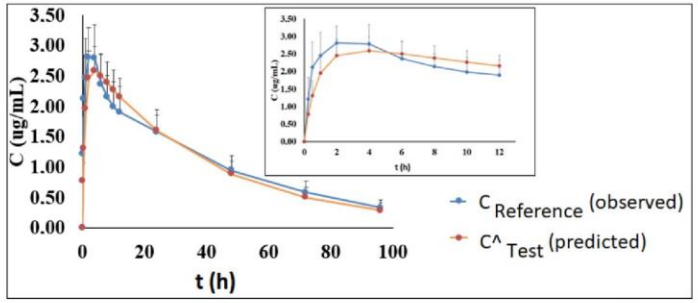

Figure 5. Plasma profiles of test and reference products

CONCLUSION

This study demonstrated that the described biphasic test method provided a discriminative and in vivo predictive power for LTG tablet formulations.

REFERENCES

1. Incecayir, T., et al. Comparison of plasma and saliva concentrations of lamotrigine in healthy volunteers. Arzneimittelforschung, 2007, 57: p. 517-521.
2. Wagner J.G. Estimation of theophylline absorption rate by means of the Wagner-Nelson equation. Journal of Allergy and Clinical Immunology, 1986, 78: p. 681-688.

ACKNOWLEDGEMENTS

The authors would like to thank Sanovel Pharmaceuticals (Istanbul, Turkey) for kindly providing LTG drug substance.

PREPARATION AND EVALUATION OF ALPHA TOCOPHEROL/ CYCLODEXTRIN COMPLEXES

[1,2]Adatepe, Ş., [1]Demirel M.

1 Anadolu University, Faculty of Pharmacy, Department of Pharmaceutical Technology, Eskişehir, Turkey mdemirel@anadolu.edu.tr

2 University of Health Sciences, Gulhane Faculty of Pharmacy, Department of Pharmaceutical Technology, Ankara, Turkey seyma.adatepe@sbu.edu.tr (Presenter)

Introduction:

The alpha tocopherol (ATC) uses commonly in cosmetic products. It has antioxidant, antibacterial, skin regenerating and antiaging properties, but it is sensitive to light, oxygen and heat. It may be irritating for skin in high concentrations. ATC must be in low concentration with high efficiency in an ideal cosmetic product. Therefore in our study, ATC: cyclodextrin complexes were prepared with hydroxypropyl beta cyclodextrin (HPBCD) and randomly methylated beta cyclodextrin (RAMEB) [1,2].

Materials and Methods:

ATC (Fluorochem, UK), HPBCD (Applichem, Germany) and RAMEB (CTD, Inc. USA) were used as received for preparing ATC:CD complexes. All other chemicals were in analytical grade. The inclusion complexes were prepared by freeze drying method [3]. A modified HPLC method was used for the determination of ATC [4]. SEM (Zeiss, Supratm 50 VP, Germany), DSC (Shimadzu DSC-60, Japan) 1H-NMR (Bruker Ultra Shield CPMAS NMR) analyses, dissolution rate, antioxidant activity and stability studies were performed.

Results:

SEM (Fig.1), DSC (Fig.2), 1H-NMR (Fig.3), FT-IR (Fig.4) analyses results, dissolution rate studies (Fig. 5), antioxidant activity (Fig.6), stability results (Fig.7) were presented. (C1: ATC: HPBCD Complex, C2: ATC: RAMEB Complex)

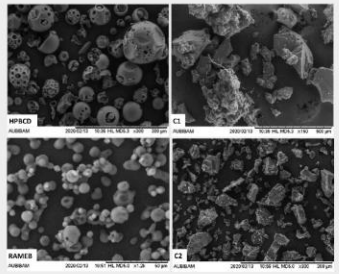

Fig.1. SEM

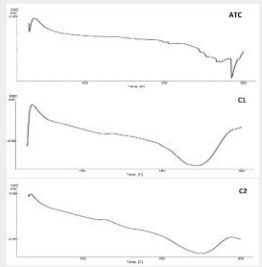

Fig.2. DSC

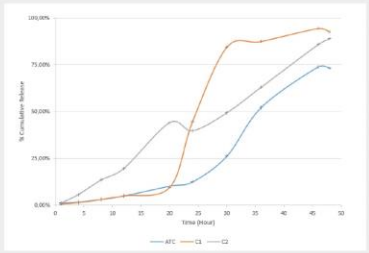

Fig.5. Dissolution Rate (Mean±SE, n=6)

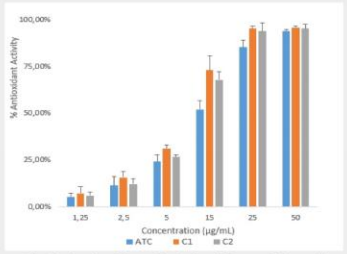

Fig.6. Antioxidant Activity (Mean±SE, n=6)

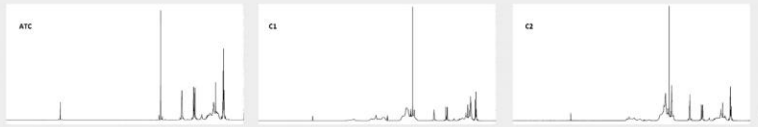

Fig.3. ^{1}H-NMR

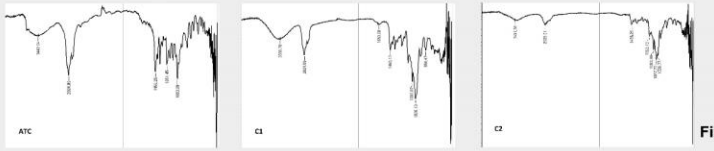

Fig.4. FT-IR

Code	Storage condition	% ATC					
		Initial	12. Day	20. Day	30. Day	60. Day	90. Day
ATC	2-8°C	100	101,09 ±1,21	95,47 ±0,28	93,46 ±2,09	92,67 ±1,14	88,62 ±1,54
	25° C Sunlight		9,57 ±0,08	9,34 ±0,43	9,25 ±0,07	9,08 ±0,20	8,21 ±0,62
	25° C Dark		96,92 ±0,14	94,10 ±0,49	92,60 ±1,50	92,74 ±1,80	74,12 ±1,44
	40° C		94,23 ±1,14	93,44 ±0,12	91,10 ±0,84	87,82 ±1,37	75,62 ±2,35
C1	2-8°C	100	96,90 ±0,93	96,06 ±0,12	95,86 ±0,75	94,97 ±0,99	93,77 ±0,23
	25° C Sunlight		8,65 ±0,29	8,68 ±0,03	8,36 ±0,26	8,08 ±0,07	7,83 ±0,19
	25° C Dark		96,81 ±0,59	94,37 ±0,87	94,37 ±0,11	91,92 ±0,46	86,51 ±1,20
	40° C		95,40 ±0,26	93,70 ±1,13	93,42 ±0,36	87,03 ±0,13	74,27 ±4,85
C2	2-8°C	100	104,05 ±0,32	101,69 ±1,16	100,33±2,16	99,23 ±1,43	99,00 ±0,43
	25° C Sunlight		9,43 ±0,36	8,53 ±1,29	8,36 ±0,45	8,22 ±0,24	7,32 ±0,85
	25° C Dark		102,31 ±1,08	98,18 ±0,27	97,87 ±0,75	97,44 ±0,31	91,48 ±0,07
	40° C		97,81 ±0,48	97,79 ±0,56	96,93 ±1,10	88,35 ±0,44	75,48 ±3,04

Fig.7. Stability Results (Mean ±SE, n=3)

Discussion:

α-TC:CD complexes have been successfully prepared in solid form by lyophilization method, and it has been shown that inclusion complexes are formed in DSC, SEM, FT-IR, 1H-NMR characterization studies [5,6,7,8]. Compared to pure ATC, solubility, dissolution rate and antioxidant activity were increased in complexes. ATC: RAMEB was found to be more stable than other complex at different storage conditions (2-8 °C refrigerator, 25 °C dark and sunlight, 45 °C etuv) during 3 months.

References:

[1] Konger, R. (2006). J. Invest. Derm., 126, 1447–1449

[2] Lupo, M.P. (2001). Clin. Dermatol., 19(4), 467-473

[3] Güleç, K., & Demirel, M. (2016). Curr. Drug Deliv., 13(3), 444-451

[4] Gupta S.K., Ramya M.G., Akki R., Kathırvel S., Naik V.V. (2013). J. Pharm. Pharm. Sci., 5(3), 921-925.

[5] Sobrinho, J. vd. (2011). Quim. Nova, 34(9), 1534-1538.

[6] Li, B. vd. (2013). Carbohydr. Polym. , 92, 2033– 2040.

[7] Demirel, M., Yurtdaş, G., & Genç, L. (2011). J. Incl. Phenom. Macrocycl. Chem., 70, 437-445.

[8] Singireddy, A., & Subramanian, S. (2016). Part. Sci. Technol., 34, 341-346.

SEMISOLID NLC FORMULATIONS FOR COSMETIC USE: EVALUATION OF MECHANICAL PROPERTIES

[1] Cakir, K., [2] İnal, Ö., [2] **Badilli, U.**

[1] Cakir Pharmacy, Ankara, Turkey

[2] Ankara University, Faculty of Pharmacy, Department of Pharmaceutical Technology, Ankara, Turkey,

unuman@pharmacy.ankara.edu.tr

INTRODUCTION

Nanostructured lipid carriers (NLCs), the second generation of lipid nanoparticles, have been received great attention as cosmetic delivery systems (1). Semisolid lipid nanoparticle dispersions are the final product for patient use at the end of the single-step production process and thus they are cost and time effective (2).

In this study, four different herbal oils that have anti-aging effects were used as liquid lipids for the preparation of semisolid NLC dispersions and the mechanical properties of the formulations were evaluated.

MATERIALS & METHODS

Preparation of Semisolid NLC Dispersions

Semisolid NLC formulations were prepared by high shear homogenization and ultrasonication method (Fig 1). Compritol 888 ATO (C-ATO) was used as solid lipid and pomegranate seed (P), argan (A), grape seed (G) and coconut (C) oils were used as liquid lipids.

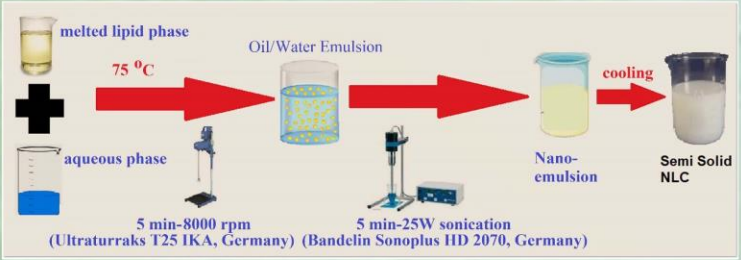

Figure 1. Preparation of semisolid NLC dispersions

In vitro Characterization of Semisolid NLC Dispersions

- Particle size, polydispersity index (PDI) and zeta potential values of the formulations were analyzed by using Malvern Zetasizer Nano ZS. Formulations were diluted with ultrapure water before analysis.

- Texture Profile Analysis (TPA) was studied by using TA.XT Texture Analyzer (Stable, UK) for evaluating mechanical properties of formulations.

RESULTS

Table 1. Compositions and in vitro characterization results of semisolid NLC dispersions

	C-ATO (g)	P (g)	A (g)	G (g)	C (g)	P-188 (g)	Water (ml)	Particle Size (nm) ± SD	PDI ± SD	Zeta Potential (mV) ± SD
CP 15	1.8	0.45	0	0	0	0.375	15	322.9±4.518	0.267±0.017	-29,4±0,661
CA 15	1.8	0	0.45	0	0	0.375	15	227.5±4.167	0.233±0.011	-29,4±0,404
CG 15	1.8	0	0	0.45	0	0.375	15	303.2±6.325	0.332±0031	-29,7±0,517
CC 15	1.8	0	0	0	0.45	0.375	15	288.2±5.340	0.298±0.026	-30,7±0,444
CP 20	2.4	0.6	0	0	0	0.375	15	330.1±3.788	0.273±0.038	-33,1±0,698
CA 20	2.4	0	0.6	0	0	0.375	15	259.9±6.998	0.267±0.004	-30,7±0,230
CG 20	2.4	0	0	0.6	0	0.375	15	419.7±7.969	0.343±0.020	-29,7±0,620
CC 20	2.4	0	0	0	0.6	0.375	15	304.6±7.932	0.239±0.011	-28,7±0,630

C-ATO: Compritol ATO 888; P-188: Poloxamer 188; P: Pomegranate seed oil; A: Argan oil; G: Grape seed oil; C: Coconut oil

Table 2. Texture profile analysis parameters of semisolid NLC dispersions

Code	Hardness (N)	Compressibility (N.sec)	Adhesiveness (N.sec)	Cohesiveness	Elasticity
CP15	21.98	54.24	29.47	0.616	0.993
CA15	61.31	116.01	54.74	0.558	0.976
CG15	64.87	134.99	71.16	0.490	0.995
CC15	77.72	139.13	85.78	0.683	1.000
CP20	50.07	114.67	59.83	0.665	0.976
CA20	147.28	313.17	136.31	0.601	0.990
CG20	128.32	256.75	87.03	0.557	0.996
CC20	142.39	251.68	75.82	0.392	0.990

DISCUSSION

Mean particle size, PDI and zeta potential results were given in Table 1. Mean particle size values between 227.5±4.167 and 419.7±7.969 nm, PDI values between 0.233±0.011 and 0.343±0.020 and zeta potential values approximately -30 mV were found.

Lower particle sizes were obtained with the formulations that contains 15% total lipid amount. Among the liquid lipids, the formulations produced with argan oil have the lowest particle size compared to other liquid lipids.

In TPA analysis, lower hardness and compressibility indicates the ease of application while lower numerical value of elasticity and higher adhesiveness indicates enhanced retention of formulation on the skin. The hardness, compressibility and adhesiveness of the formulations prepared with pomegranate seed oil were significantly lower than the formulations prepared with other herbal oils (Table 2).

CONCLUSION

Even the particle size of CA15 is the lowest among the formulations, according to hardness, compressibility and elasticity properties, CP15 and CP20 formulations prepared with pomegranate seed oil seems to have best values for ease of application and ease of spreading onto the skin. Considering all the mechanical parameters given above, these semisolid NLC formulations was concluded as the most appropiate choice for cosmetic applications.

REFERENCES

1. Souto EB, Muller RH (2008). International Journal of Cosmetic Science, 30: 157–165.
2. Badıllı U, Turk CT, Amasya G, Tarımcı N (2017). Current Drug Delivery, 14(3): 386 – 393.

JUNE 22-25, 2021 ANKARA, TURKEY
ISOPS 13th International SYMPOSIUM ON PHARMACEUTICAL SCIENCES

PREPARATION AND *IN VITRO* CHARACTERIZATION OF LIPID-COATED NANOPARTICLES CONTAINING CARBOPLATIN AND DECITABINE

[1]Esim, O., [2]Hascicek, C.

[1] Ankara University, Department of Pharmaceutical Technology, Ankara, Turkey, gun@ankara.edu.tr

[2] Ankara University, Department of Pharmaceutical Technology, Ankara, Turkey, cogan@pharmacy.ankara.edu.tr

Introduction

Silencing of critical tumor suppressor genes by DNA hypermethylation is the major epigenetic cause of chemoresistance of cancer cells. DNA methyltransferase inhibitors, such as decitabine (DEC), allow silenced critical tumor suppressor genes to be re-expressed by demethylation [1]. In this regard, the combination of DNA methyltransferase inhibitors and conventional chemotherapeutics is thought to be promising approach for modulating drug resistance by sensitizing of cancer cells. The aim of this study is to develop carboplatin (CRB) and DEC loaded lipid-coated albumin nanoparticles for the treatment of platinum-resistant ovarian cancer and evaluate the physicochemical properties of the nanoformulations.

Materials

CRB, DEC, glutaraldehyde, soy phosphatidyl choline and cholesterol were purchased from Sigma-Aldrich (Saint-Louis, MO, USA). Bovine serum albumin was supplied from Amresco (Solon, OH, USA). All other chemicals used were at least of reagent grade. Water pretreated with the Milli-Q® Plus System (Milipore Corp., Molsheim, France) was used in all experiments.

Methods

The production method of lipid-coated nanoparticles consisted of two steps (Fig. 1) [3]. In the first step CRB-loaded albumin-based nanoparticles were prepared by desolvation methods [2]. Then these nanoparticles were coated with a DEC-containing lipid layer. To optimize the lipid-coating procedure, the effects of various lipid:nanoparticle ratios, lipid film compositions and rehydration medium volumes on the physicochemical properties of the nanoparticles were examined (Table 1). Developed nanoparticle formulations were evaluated in terms of drug loading (DL), particle size and size distribution (PDI), surface charge, particle morphology and thermal behaviors (Table 2).

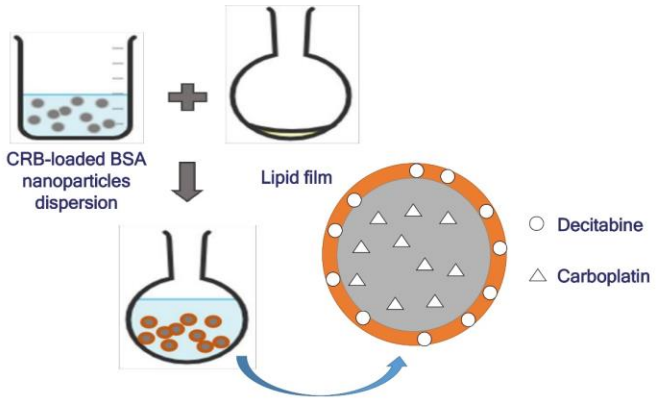

Figure 1. Schematic presentation of preparation of lipid-coated nanoparticles [3]

Table 1. Formulation composition of nanoparticles

Code	Lipid/nanoparticle (w/w)	Lipid composition (Phosphatidylcholine/Cholesterol) (w/w)	Dispersion media volume (ml)	CRB (mg)	DEC (mg)
LA1	1:1	1:1	10	-	-
LA2	1:1	1:0.5	10	-	-
LA3	0.5:1	1:1	10	-	-
LA4	0.5:1	1:0.5	10	-	-
LA5	1:1	1:0.5	5	5	1
LA6	1:1	1:0.5	2	5	1

Table 2. Characterization of nanoparticles

Code	Particle Size (nm)	PDI	Zeta potential (mV)	CRB leakage from core (%)	DL_{CRB} (%)	DL_{DEC} (%)
LA1	266.8±26.92	0.223±0.071	-27.6±1.70	78.14±0.943	0.296±0.012	-
LA2	220.6±21.29	0.075±0.014	-27.1±0.50	79.61±1.004	0.275±0.026	-
LA3	253.8±34.45	0.192±0.102	-25.1±4.60	76.36±0.788	0.326±0.098	-
LA4	224.7±15.65	0.078±0.032	-25.5±0.19	79.03±0.708	0.283±0.052	-
LA5	281.5±13.03	0.584±0.098	-14.7±0.73	57.98±2.597	0.340±0.030	0.853±0,088
LA6	272.3±3.787	0.298±0.036	-10.9±2.70	13.65±0.088	1.228±0.004	1.146±0.016

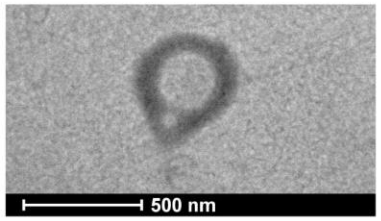

Figure 2. TEM image of CRB- and DEC-loaded lipid-coated BSA nanoparticle

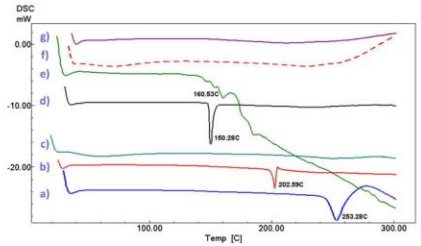

Figure 3. DSC thermogram of a)Carboplatin b) Decitabine c)BSA d)Cholesterol e)Soy phosphatidyl choline f) CRB-loaded BSA nanoparticles g) CRB- and DEC- loaded lipid-coated nanoparticle

Results and Discussion

To obtain an intact lipid shell onto the CRB-loaded BSA nanoparticles and proper particle size, particle size distribution, surface charge and encapsulation efficiency varying parameters were evaluated.

When lipid: nanoparticles ratio was investigated and it was found that there was not an intact lipid structure on nanoparticles for 0.5:1 ratio; however there was a smooth lipid envelop for 1:1 ratio.

In order to determine the optimum lipid composition, two different soy phosphatidyl choline:cholesterol ratios were explored and 1:0.5 ratio was selected for further studies due to the smaller particle size and narrower particle size distribution.

Lastly lower dispersion media volumes were investigated to decrease the CRB leakage from the core nanoparticles during the lipid coating procedure. Lower dispersion media volumes resulted in decreased CRB leakage and 2 ml was found as optimum.

Multidrug-containing lipid-coated nanoparticles were obtained 1:1 (w:w) lipid:nanoparticle ratio, 1:0.5 (w:w) soy phosphatidyl choline:cholesterol ratio and 2 ml rehydration medium volume. The optimum nanoparticle formulation showed 272.3 nm particle size, 0.298 PDI, -10.9 surface charge and 1.228% and 1.146% drug loading for CRB and DEC, respectively.

The morphological structure of the optimum nanoparticles formulation was explored by transmission electron microscopy (TEM). As seen in Fig. 2, the nanoparticles showed a core-shell structure composed of a spherical core nanoparticle and a dim ring surrounding the core nanoparticles.

The thermal behavior of the nanoparticles were investigated by differential Scanning calorimetry (DSC) analysis.The characteristic endothermic peaks at 253.28 and 202.59 °C were seen in the thermogram of pure carboplatin and decitabine, respectively. On the other hand, these peaks were not observed in the thermogram of nanoparticle formulation, which can be attributed to the amorphous states of drugs into the nanoparticles (Fig. 3).

Conclusions

The thin film hydration method-based two-step preparation method was successfully applied to the DEC-loaded lipid coating of CRB-loaded albumin nanoparticles with desired physicochemical properties and relatively high encapsulation efficiencies.

Acknowledgements

This study was supported by a grant of TUBITAK (SBAG-116S395)

References

1.Nguyen HT, Tian, G, Murph MM (2014). Molecular Epigenetics in The Management Of Ovarian Cancer: Are We Investigating A Rational Clinical Promise?, Frontiers in Oncology, 4:1-12.

2.Esim, O, Gumustas, M, Hascicek, C, Ozkan, SA (2020). A novel stability-indicating analytical method development for simultaneous determination of carboplatin and decitabine from nanoparticles. Journal of Separation Sciences, 43(17):3491-3498.

3.Esim O, Hascicek C (2021). Lipid-Coated Nanosized Drug Delivery Systems for an Effective Cancer Therapy, Current Drug Delivery, 18 (2):147-161.

JUNE 22-25, 2021 ANKARA, TURKEY
13th International SYMPOSIUM ON PHARMACEUTICAL SCIENCES

DEVELOPMENT AND CHARACTERIZATION OF BUCCAL FILM CONTAINING HYDROCORTISONE NANOSUSPENSIONS

[1,2]Çulcu, Ö., [1]Saar, S., [1]Tuğcu-Demiröz F., [1]Tirnaksiz F.

[1] Gazi University, Department of Pharmaceutical Technology, Ankara, Turkey, fatmanur@gazi.edu.tr, ozlem.culcu@gazi.edu.tr

[2] Agri Ibrahim Cecen University, Department of Pharmaceutical Technology, Agri, Turkey

JUNE 22-25, 2021 ANKARA, TURKEY

13th International SYMPOSIUM ON PHARMACEUTICAL SCIENCES

ANKARA UNIVERSITY FACULTY OF PHARMACY

INTRODUCTION

Aphthous ulcers are oral mucosal inflammatory ulcers that occur in the oral cavity and antibiotics, antiseptics, and topical corticosteroids are often used for treatment (1).

Hydrocortisone (HC) is an anti-inflammatory compound with low solubility in water and is used for treatment of aphthous ulcers (1).

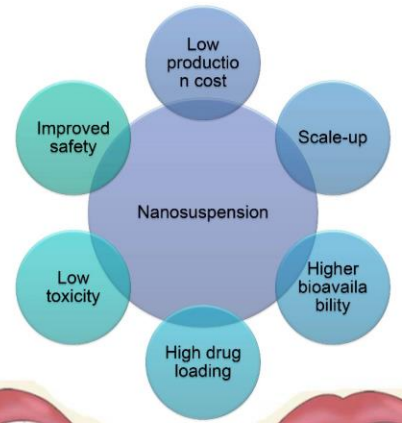

The low water solubility of drug substances limits drug administration due to low bioavailability.

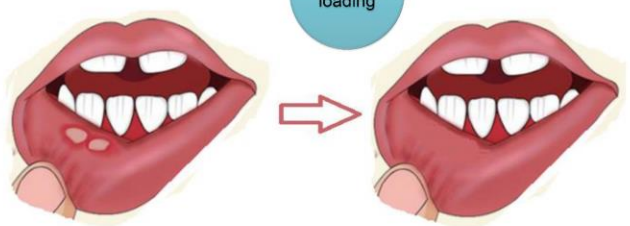

Mucoadhesive films have many advantages such as drug localization, flexibility, handling and ease of use.

Nanosuspensions allows poorly water-soluble compounds to form nano-sized particles in an aqueous formulation, providing a more effective treatment (2).

The aim of this study is to increase the solubility of HC by preparing a nanosuspension (NS) formulation and to load it into the film formulation to be used in the treatment of aphthous ulcers.

In this way, the bioavailability of the drug will increase with the nanosuspension formulation and the film formulation will provide ease of application to the patients.

METHODS

Hydrocortisone loaded nanosuspension (HC-NS) was prepared by media milling method using different concentrations hydroxypropyl methylcellulose E4 (HPMC) and polyvinylpyrrolidone K90 (PVP) as stabilizers(3).

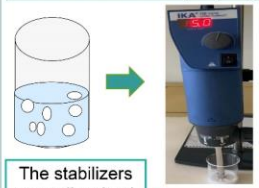

The stabilizers were dissolved in distilled water and the HC was dispersed in the stabilizer solution.

Dispersion mixed with Ultraturrax at 15,000 rpm for 5 minutes.

NS were prepared by adding 0.5mm sized zirconium oxide beads at 350 rpm using different processing times (0.5, 1 and 2 hours).

After the process was completed, nanosuspensions were separated using 200 mesh size sieve.

The zeta potential (ZP), particle size (PS) and polydispersity index (PDI) of NSs were measured with Malvern ZetaSizer.

The solvent casting method was used to develop a buccal film formulation containing the HC-NS.

Pectin (3%) was dispersed into the optimum NS.

Plasdone K12 and glycerin (3%) were added.

Polymer mixtures are poured into petri dishes and dried in the oven.

Characterization of HC-NS Loaded Film Formulation

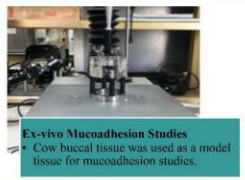

Ex-vivo Mucoadhesion Studies
- Cow buccal tissue was used as a model tissue for mucoadhesion studies.

Mechanical Properties
- Texture Analyzer was used to determine the mechanical properties.

Moisture Content
- Moisture content was determined with a moisture analyzer (Sartorius Moisture Analyzer, Germany).

RESULTS

Stabilizer Type	Process Time (h)	0,25% Stabilizer Concentration			0,5% Stabilizer Concentration		
		ZP (mV)	PS (nm)	PDI	ZP (mV)	PS (nm)	PDI
PVP	0,5	-16.9±0,404	278,9±21,41	0,449±0,052	-19±1,20	230,7±25,62	0,478±0,048
	1	-6,08±0,870	444,2±17,02	0,576±0,070	-17,6±1,06	232,9±52,49	0,451±0,132
	2	-6,63±0,350	325,5±6,691	0,386±0,019	-28,9±1,78	148,9±3,134	0,301±0,006
HPMC	0,5	-14±6,29	482,7±4,981	0,646±0,054	-6,23±0,752	322,3±72,66	0,510±0,065
	1	-10,2±1,69	441,6±38,30	0,570±0,014	-5,47±0,929	266,1±11,71	0,443±0,019
	2	-16,1±0,586	280,1±17,73	0,458±0,055	-4,45±3,70	210,0±25,80	0,417±0,007

Table 1. Characterization results of the nanosuspension formulations

Characterization Results of HC-NS Loaded Film Formulation

- The mechanical properties of the HC-NS loaded film formulation were 19.8±0.02 mPa, and the elongation at break value was 17.7±4.02%.
- Work of mucoadhesion was 0.067±0.015 mJ/cm² in buccal tissue.
- Moisture content of HC-NS loaded film formulation was 14.56%.

DISCUSSION

Process time and the choice of stabilizer used in the production of nanosuspensions affected ZP, PDI and PS.

Nanosuspensions with smaller PS and PDI values were obtained by increasing the stabilizer concentration in both polymers.

The optimum formulation of HC-NS was obtained with ***0.5% PVP concentration*** and a ***two hour process time***.

The buccal film formulation containing HC-NS has been successfully developed.

Prepared films should be stored airtight to prevent moisture loss and maintain elasticity.

The HC-NS loaded film formulation was found suitable for buccal application in terms of mechanical and ex-vivo mucoadhesive properties.

REFERENCES

1. Sanjana, A., Ahmed, M. G., & Bh, J. G. (2021). *Journal of Oral Biology and Craniofacial Research*, *11*(2), 269-276.

2. Liu, Q., Mai, Y., Gu, X., Zhao, Y., Di, X., Ma, X., & Yang, J. (2020). *Journal of Drug Delivery Science and Technology*, 55, 101371.

3. Oktay, A. N., Ilbasmis-Tamer, S., Karakucuk, A., & Celebi, N. (2020). *Journal of Drug Delivery Science and Technology*, *57*, 101690.

PREPARATION AND EVALUATION OF LYSOZYME LOADED POLYCAPROLACTONE MICROPARTICLES USING THE FULL FACTORIAL DESIGN

[1]Devrim, B., [2]Erdinç, N.

[1]Ankara University, Department of Pharmaceutical Technology, Ankara, Turkey, bdevrim@pharmacy.ankara.edu.tr
[2]Turkish Medicines and Medical Devices Agency, Ankara, Turkey, nilhanecz@gmail.com

INTRODUCTION

The growing problem of multidrug-resistant bacteria has encouraged the search for therapeutic alternatives to conventional antibiotics. To this end, there is a growing interest in the use of antimicrobial peptides (1). Lysozyme is a monomeric protein that can be used in the treatment of microbial infections due to its antimicrobial activity, but the relatively narrow antimicrobial spectrum, instability and easy inactivation make the practical application of free lysozyme quite limited (2). Considering these reasons, poly-ε-caprolactone (PCL) microparticles of lysozyme were prepared using the full factorial design in this study.

MATERIALS AND METHODS

Lysozyme, egg white was obtained from Vivantis (Oceanside, CA). Poly-ε-caprolactone (PCL), poly(vinyl alcohol) (PVA) and dichloromethane (DCM) were from Sigma (Germany).

Lysozyme loaded microparticles were prepared by w/o/w double emulsion solvent evaporation method (Figure 1). Based on a 2^4 full factorial design, different lysozyme concentrations, DCM volumes, PVA volumes and homogenisation rates were used as independent variables (Table 1). Compositions of lysozyme loaded PCL microparticles were given in Table 2.

Figure 1. Preparation of lysozyme loaded PCL microparticles

Table 1. Selected experimental factors for preparation of lysozyme loaded PCL microparticles at the desired levels

Independent variables	Level	
	-1	+1
Lysozyme concentration (mg)	5	10
Volume of DCM (ml)	3	5
Volume of PVA solution (ml)	20	30
Homogenization rate (rpm)	8000	13500

Table 2. Composition of lysozyme loaded PCL microparticles

Formulation code	Lysozyme concentration (mg)	Volume of DCM (ml)	Volume of PVA solution (ml)	Homogenization rate (rpm)
F1	7.5	4	25	9500
F2	5	3	30	13500
F3	5	5	30	8000
F4	5	3	20	13500
F5	10	3	20	8000
F6	10	3	30	13500
F7	7.5	4	25	9500
F8	5	3	30	8000
F9	10	5	30	13500
F10	5	3	20	8000
F11	10	3	20	13500
F12	5	5	20	8000
F13	7.5	4	25	9500
F14	7.5	4	25	9500
F15	5	5	30	13500
F16	10	5	20	13500
F17	10	5	20	8000
F18	10	5	30	8000
F19	5	5	20	13500
F20	10	3	30	8000

Partic[illegible] size analy[illegible]ency (%) was calculated using following equation:

Encapsulation efficiency (%)=(Calculated drug concentration)/(Theoretical drug concentration)×100

RESULTS AND DISCUSSION

The effects of DCM volume, PVA volume and homogenization rate on particle size were found to be significant ($p<0.05$). Otherwise, the effects of lysozyme concentration and PVA volume on encapsulation efficiency is significant ($p<0.05$).

a)

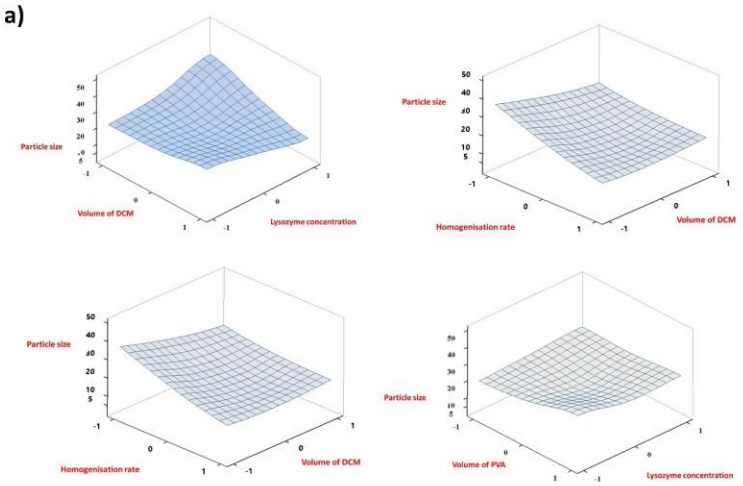

b)

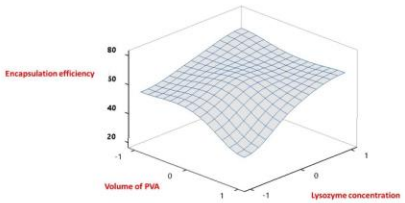

Figure 2. 3D response surface plots for the effect of the independent variables on particle size (a) and encapsulation efficiency (b)

CONCLUSION

The PCL microparticles containing lysozyme were prepared successfully by using w/o/w double emulsion solvent evaporation method. As a result, lysozyme loaded PCL microparticles can be used in the treatment of microbial infections.

References:

1.Tapan et al., (2011). Experimental Lung Research, 37:9, 536-541.
2. Wu et al., (2017). Carbohydrate Polymers, 155, 192–200.

JUNE 22-25, 2021 ANKARA, TURKEY
13th International Symposium on Pharmaceutical Sciences

INVESTIGATION OF MISCELLISATION CHARACTERISTICS OF POLYOXYL CASTOR OIL FOR VITAMIN D3 PREPARATIONS IN TURKISH DRUG MARKET

[1]Akgeyik, E., [2,3]Kaynak, MS., [4]Koçer-Gümüşel, B., [5]Gümüşel, B.

[1]Yozgat Bozok University, Science and Technology Application and Research Center (BILTEM), Yozgat, Turkey. **emrah.akgeyik@gmail.com**
[2]Anadolu University, Department of Pharmaceutical Technology, Eskisehir, Turkey. msinankaynak@gmail.com
[3]Anadolu University, Yunus Emre Vocational School of Health Services, Department of Pharmacy Services, Eskişehir, Turkey
[4]Lokman Hekim University, Department of Pharmaceutical Texicology, Ankara, Turkey, belmagumusel@yahoo.com
[5]Lokman Hekim University, Department of Pharmacology, Ankara, Turkey, bulentgumusel@yahoo.com

INTRODUCTION

Micellization in the gastrointestinal tract plays an important role, especially in the absorption of drugs with low solubility. The entrapment of drugs in micelles in the gastrointestinal tract causes significant changes in their distribution and pharmacokinetics in the body, which are important for their activities. Polyoxyl 35 castor oil (Polyoxyl Castor Oil, PCO) (**Figure 1-A**) is a nonionic surfactant and used as an emulsifying agent that increasing solubility through micelle formation in pharmaceutical dosage forms such as tablets, emulsions, creams, ointments, etc. In this study, it is aimed to determine the micelle formation and size by means of the excipient, PCO contained in cholecalsiferol preparation in the Turkish pharmaceutical market (1). Cholecalciferol **Figure 1-B**, also known as vitamin D3 and colecalciferol. It is a type of vitamin D which is made by the skin when exposed to sunlight. It is also found in some foods and can be taken as a dietary supplement.

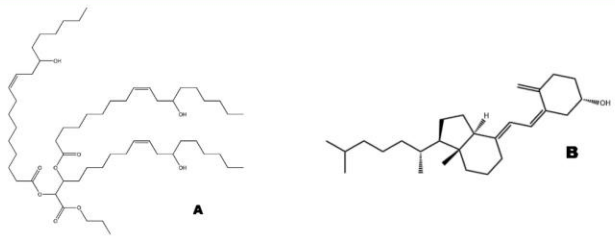

Figure 1. Molecular structure of PCO (A), Cholocalsiferol (B).

MATERIALS AND METHODS

First of all, in order to determine the micellization concentration of castor oil in pure water, samples of water:castor oil mixtures coded with "A" were prepared in pure water at the concentrations given in **Table 1** and mixed with the help of a vortex for 5 minutes. The castor oil and placebo solution, which does not contain any active substance, of the preparation named Coledan-D3 oral drops, which is available in the Turkish pharmaceutical market, was prepared by mixing. For the determination of the micellization characteristic of castor oil in the formulation; Placebo samples coded with "P", castor oil:placebo mixtures at the same concentrations given in **Table 1** were prepared and mixed in vortex for 5 minutes. The refractive indices of the prepared samples were made using the Abbe 5 Refractometer (Bellingham + Stanley, United Kingdom). Spectrophotometric analyzes of the samples were performed using the Varian Cary® 50 UV-Vis Spectrophotometer (Agilent, USA). UV spectra of the samples prepared at different concentrations in the wavelength range of 200-800nm were taken and necessary evaluations were made. KSV Instruments Cam 200 (KVS Instruments Ltd., Finland) device was used for determination of surface tension. After each sample whose surface tension is to be measured is placed in the sample injector of the device, the surface tension (γ) of each sample with the Pendant Drop Analysis method is calculated by using the software named "KSV CAM Optical Contact Angle and Pendant Drop Surface Tension Software (Ver 3.99)" that comes with the device. The obtained surface tension values were plotted against the concentration and the critical micelle concentrations were determined from this graph. Dynamic light scattering method (Dynamic Light Scattering, DLS), also known as photon correlation spectroscopy (Photon Correlation Spectroscopy, PCS) or semi-elastic light scattering (Quasi-Elastic Light Scattering, QELS), was used to determine the micelle sizes of our samples containing Campherol EL at different concentrations. Malvern Zetasizer Nano Series Nano ZS (Malvern, United Kingdom) device was used and the average particle (micelle) size (nm) of each sample was determined.

REFERENCES:
1. Hale GM, Querry MR. Optical Constants of Water in the 200-nm to 200-microm Wavelength Region. Applied optics 1973;12:555-63.
2. Priev A, Zalipsky S, Cohen R, Barenholz Y. Determination of critical micelle concentration of lipopolymers and other amphiphiles: Comparison of sound velocity and fluorescent measurements. Langmuir 2002;18:612-17.
3. Rowe RC, Sheskey PJ, Owen SnC, *Handbook of Pharmaceutical Excipients*. 2006, Pharmaceutical Press and American Pharmacists Association: Publications division of the Royal Pharmaceutical Society of Great Britain.

RESULTS

Refractive Index Determinations

The refractive indices of the prepared samples were determined by the Abbe 5 Refractometer device and the refractive index of A samples were found to be 1.333. This value is accepted as a standard measurement and It is compatible with the refractive index published by Hale et al. (1). "P" samples were placed separately on the prism on the device and their refractive indexes were determined by illuminating the chrome-plated reflector with daylight (in the range of 380-740 nm). While the refractive index of our placebo solution without surfactant was found to be 1.371, the refractive index of our samples with added surfactant was found in the range of 1.372-1.373 depending on the increase in surfactant concentration. The refractive index of the product named Coledan D3 containing polyoxy 35 castor oil was found to be 1.375. These values were used as reference values in the dynamic light scattering studies of our samples.

Spectrophotometric Analysis

UV spectrum graphics of the obtained spectra are given in **Figure 2**. The absorbance values obtained from the UV spectra of the samples prepared at increasing concentrations were determined and used as a reference value in the dynamic light scattering studies of our samples. It is seen in Figure 1 that as the concentration of PCO increases, the absorbance values at wavelengths where the samples show maximum absorbance increase.

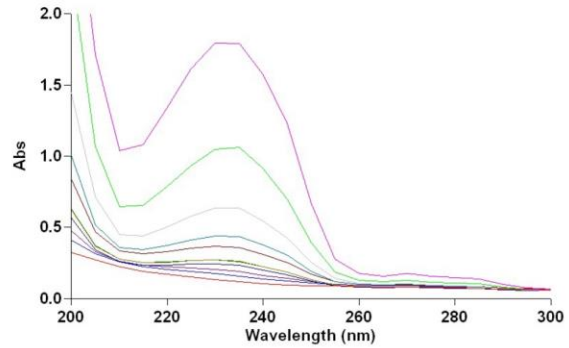

Figure 2. UV spectrum curves of "A" coded samples.

RESULTS

Surface Tension Analysis and Determination of Critical Micellar Concentration

For the determination of the critical micelle concentration of polyoxy 35 castor oil in distilled water and placebo; The surface tension values of the A and P coded samples obtained using the pendant drop method were plotted against the concentration **Figure 3** and **Figure 4**. On the graph obtained, two regions where the curve is linear for the A samples were determined and the trend lines of these two regions were drawn (**Figure 3**). The intersection point of these two trend lines, or in other words the first point where the decreasing curve reaches a plateau, shows us the critical micellar concentration of PCO dispersed in pure water. The critical micellar concentration of PCO in distilled water was determined to be approximately 0.010-0.015%. In the literature reviews, it is observed that the critical micellar concentration of PCO in pure water is given as 0.009%, 0.010% and 0.02% in various studies (2, 3). When **Figure 4** is examined for the determination of the critical micelle concentration of PCO in the placebo solution, it is striking that the curve has two turning points. With the addition of low concentrations of surfactant, there were very small changes in surface tension, while the concentration value at which micelles formed was between 0.075-0.100%, which is the second turning point value of the curve (P8 sample).

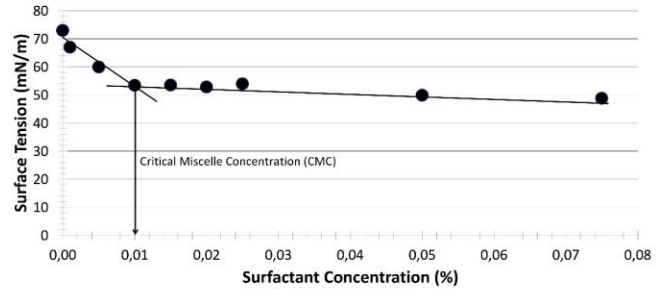

Figure 3. Concentration - surface tension graph of the samples prepared by adding surfactant in pure water

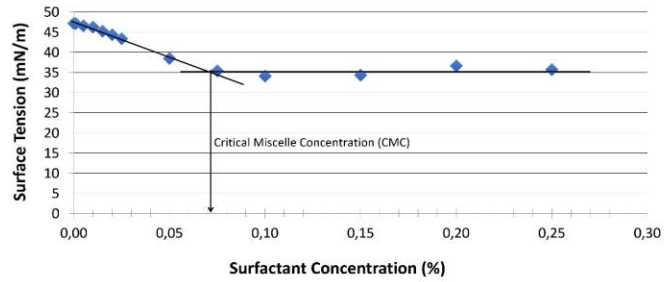

Figure 4. Concentration - surface tension graph of the samples prepared by adding surfactant in placebo solution

RESULTS

Dynamic Light Scattering Analysis

Micelle size results obtained from dynamic light scattering studies are given in Table 3. There is 2% polyoxy 35 castor oil in the product named Coledan-D3 oral drops available in the Turkish pharmaceutical market. For this reason, the micelle size results of this product are shown on the table against this concentration value so that the comparison can be made more visually.

Table 3. Micelle size values (nm) of the prepared "A" and "P" samples and the Commercial Product

Concentration (%)	0,001	0,005	0,010	0,015	0,020	0,025	0,050	0,075	0,100	0,150	0,200	0,250	0,500	0,750	1,000	1,500	2,000	2,500	3,000	4,000
A Coded Samples	276	198	225	15,42*	13,5	13,3	12,5	12,8	21,6	12,7	16,9	10,8	17,59	14	17,6	13,3	10,9	13,4	13,4	13,9
P Coded Samples	273	353	565	372,4	127	244	201	196	295	222	212	307	53,46*	336	54	44,6	41,6	50	46	44,8
Commercial Product																	41.55			

CONCLUSIONS

With surface tension studies, it was found that PCO started to miscellisation in the concentration range of 0.010-0.020% in distilled water and in the concentration range of 0.075-0.100% for placebo solution. While dynamic light scattering studies support our results for pure water, they show that micelles start after 0.5% concentration in placebo. In addition, in studies with commercial product, the refractive index of the product was found to be 1.375, the surface tension was 30.99 mN/m, and the mean micelle size was 41.55nm. All these findings show us that PCO in commercial product forms micelles with the usage concentration in the preparation. The surface tension of the product is 30.99mN/m and the average micellar size is 41.55 nm and it is equal the concentration of 2% PCO.

LACOSAMIDE LOADED MICRONEEDLES AS NASAL DRUG DELIVERY SYSTEMS

[1,2]Aykaç, K., [1]Başaran, E.

[1]Anadolu University, Faculty of Pharmacy, Department of Pharmaceutical Technology, , Eskişehir, Turkey, ebcengiz@anadolu.edu.tr

[2]Erzincan Binali Yıldırım University, Faculty of Pharmacy, Department of Pharmaceutical Technology, Erzincan, Turkey, kadir_aykac@anadolu.edu.tr

INTRODUCTION

Epilepsy is one of the most common neurological disorder mostly characterized with seizures due to the abnormal induction of neurons [1]. Lacosamide, an antiepileptic drug has low transition rate into the brain because of blood brain barrier (BBB) [2]. In our study Carboxymethyl cellulose sodium salt (CMC) based microneedles were formulated for nasal application of Lacosamide to overcome the BBB by the help of olfactory pathway with less invasive way [3].

MATERIALS AND METHODS

Lacosamide (gifted by Santa Farma, Turkey), Carboxymethyl cellulose sodium salt (CMC) and hydroxylpropyl gamma cyclodextrin (HPGCD) (Sigma-Aldrich, Germany). All other chemicals were in analytical grade. Micro-molding method was used for the preparation of CMC microneedles [4]. SEM (Zeiss Ultra Plus FE-SEM, Germany), DSC (DSC-60, Shimadzu USA), FT-IR (IR Affinity-1S Shimadzu, Japan), 1H-NMR (Fourier 300 NMR Bruker, USA) analyses were performed. A modified HPLC method was used for the determination of Lacosamide [5].

RESULTS AND DISCUSSIONS

Water soluble microneedles were prepared successfully with micro-molding method and API amounts, *in vitro* release, SEM, FT-IR, DSC and 1H-NMR analyses results were presented in Table 1 and Figure 1-Figure 5 respectively.

Table 1. Compositions of microneedles (Mean ± SE, n=3)

Code	CMC (%)	HPGCD (%)	Lacosamide Practical (%)
CL0	6.0	2.0	-
CL1	6.0	2.0	0.6 ± 0.0
CL2	6.0	2.0	1.1 ± 0.0
CL3	6.0	2.0	1.6 ± 0.0

In DSC analyses Lacosamide showed melting point at 149 °C, while CMC showed no endothermic melting peaks in thermograms, showing the amorphous structures of the polymer (Figure 1). Lacosamide melting peak was revealed in the thermograms of the physical mixtures (marked with arrows), showing that Lacosamide and polymers have no incompatibility problems.

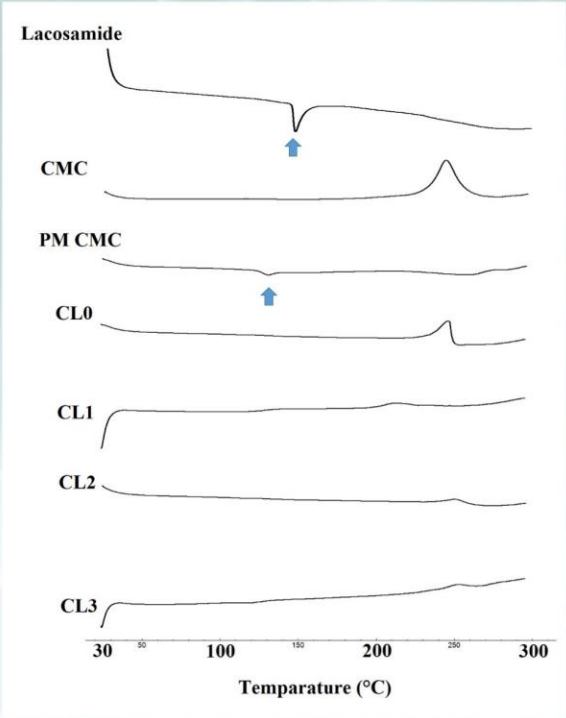

Fig. 1. DSC termograms of microneedles

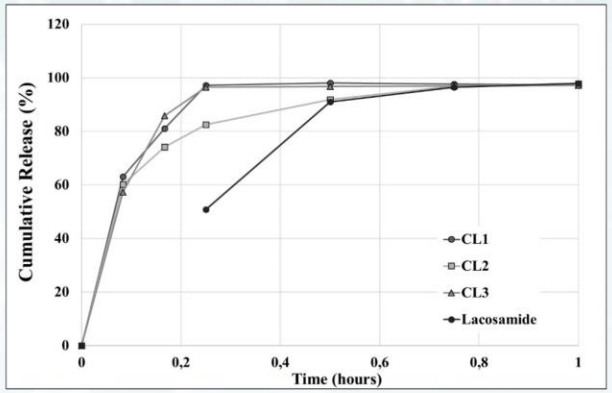

Fig. 2. *In vitro* release analyses results (Mean ± SE, n=3)

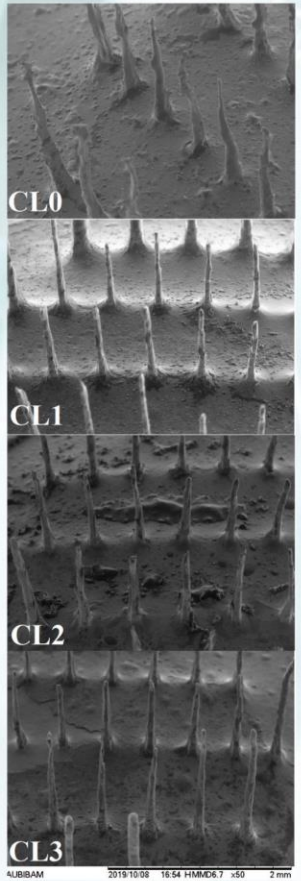

Fig. 3. SEM images of microneedles

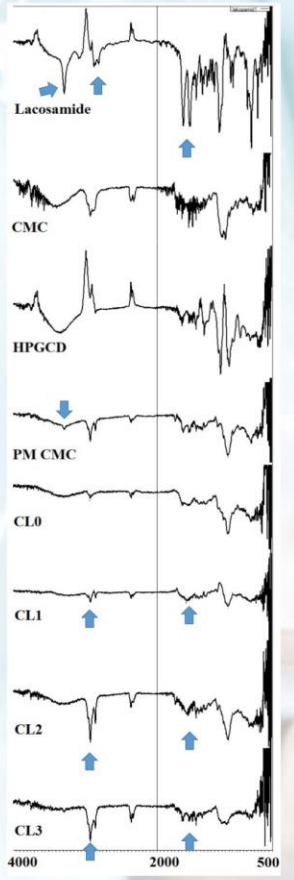

Fig. 4. FT-IR spectra of microneedles

In vitro drug release studies were performed in phosphate buffer solution (pH: 6.4) (Figure 2).

CMC based microneedles have 1300-2000 µm length and 100-250 µm diameters (Figure 3).

In FT-IR spectra, characteristic absorbtion peaks of Lacosamide were revealed in the spectrum of physical mixtures showed that Lacosamide was compatible without any interaction with both of the polymers (Figure 4).

^{1}H-NMR analyses were performed for the determination of molecular interactions between Lacosamide and polymers used in microneedle formulations. Deuterium oxide was used as a solvent. Lacosamide signals were detected in the spectra of the formulations indicating that presence of Lacosamide within the polymeric network without any chemical interactions (Figure 5).

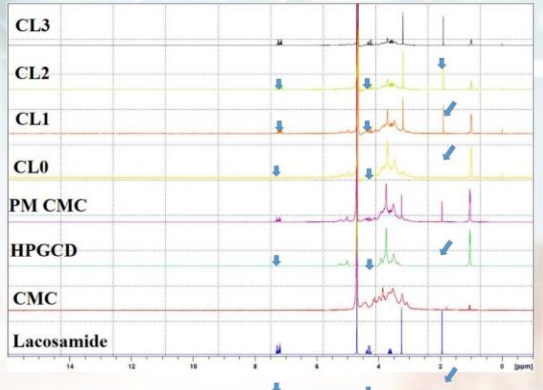

Fig. 5. ^{1}H-NMR spectra of microneedles

CONCLUSIONS

CMC based water soluble microneedles were prepared successfully for nasal application of Lacosamide by micro-molding method. *In vitro* characterization analyses results revealed the structural properties of microneedles.

In vivo studies will be performed for the determination of enhanced bioavailability of Lacosamide with the help of olfactory pathway to overcome BBB with less invasive way

ACKNOWLEDGEMENTS

DOPNA-LAB for FT-IR, ^{1}H-NMR and BIBAM for SEM Analyses.

REFERENCES

[1] Schwartzkroin PA. (2012). In: Handbook of Clinical Neurology. Elsevier. p. 13-33.

[2] Gáll Z, Vancea S. (2018). Arch Pharm Res.41(1):79-86.

[3] Appasaheb PS, Manohar SD, et al., (2013). J Adv Pharm Educ Res. 3(4):333-46.

[4] Wang M, Hu L, et al.(2017). Lab Chip. 17(8):1373-87.

[5] Sreenivasulu V, Rao DR, et al.(2011). Res J Pharm Biol Chem Sci. 2(4):1-11.

MODELING AND COMPARISON OF IN VITRO DISSOLUTION PROFILES OF NAPROXEN SODIUM TABLETS IN BIORELEVANT MEDIA

[1]Seval OLGAC, [1]Duygu YILMAZ USTA, [2]Baris DEMIRDAS, [2]Nebahat Ayse ERMAN, [1]Zeynep Safak TEKSIN

[1] Gazi University, Department of Pharmaceutical Technology, Ankara, Turkey
[2] Gazi University, Faculty of Pharmacy, Ankara, Turkey
seval.olgac@gazi.edu.tr

INTRODUCTION

In vitro dissolution tests are used to define the effect of formulation factors on bioavailability during drug development. Naproxen sodium (NS) is a widely used non-steroidal anti-inflammatory drug, which Biopharmaceutics Classification System (BCS) Class II (pKa : 4,19) [1]. The pH and composition of the dissolution medium have a great impact on its solubility. This study was aimed to compare the dissolution profiles of NS tablets using DDSolver® [2].

MATERIALS AND METHODS

Materials

Naproxen sodium was received as a gift sample from Pharmactive drug company. Reference and generic 550 mg tablets were purchased from the local market. Potassium phosphate monobasic, sodium phosphate monobasic dihydrate, hydrochloric acid were purchased from Merck, Germany. Sodium hydroxide was purchased from Sigma-Aldrich, Sweden. Sodium chloride was purchased from Merck, Denmark. Glacial acetic acid was purchased from Sigma-Aldrich, Germany, and Minisart® NY25 Syringe Filter was purchased from Sartorius, Germany. All chemicals and reagents used were of analytical grade. SIF powder was purchased from Biorelevant (United Kingdom). Lot numbers of reference and generic products are presented in Table 1.

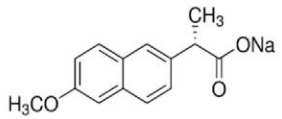

Figure 1. Chemical structures of naproxen sodium

Table 1. Lot numbers of reference and generic products

	Reference	G1	G2	G3	G4
Lot No	20D442	18001012B	20064	19061330	A087999

Methods

The solubility studies were carried out for pH 7.4 and the dose number was calculated. Dissolution studies were carried out in USP Apparatus II (Agilent Technologies 708-DS, USA) according to the USP 30. All collected samples were filtered with a 0.45 µm syringe filter and then analyzed with validated UV spectrophotometric method at 330 nm (Agilent Technologies Cary 60 UV-Vis, USA).

Apparatus	: USP Apparatus II
Medium	: pH 7.4 phosphate buffer, FaSSIF, and FeSSIF
Volume	: 900 mL
Temperature	: 37.0 °C ± 0.5 °C
Rotation Speed	: 50 rpm
Time Intervals	: 5, 10, 15, 20, 30, 45, 60, 90, and 120 min

The dissolution data analysis was performed model-independent (similarity factor (f_2)) and model-dependent using DDSolver®. The dissolution test in biorelevant media (Fasted State Simulated Intestinal Fluid (FaSSIF) and Fed State Simulated Intestinal Fluid (FeSSIF)) were performed with the generic product (G), which was determined to have the highest similarity factor calculated as a result of the dissolution tests performed in pH 7.4. The adjusted determination coefficient (r^2 adj), Akaike information criterion (AIC), and model selection criterion (MSC) were used to determine the most appropriate release model. The model with the lowest AIC, highest MSC, and r^2 value was evaluated as the most appropriate model.

RESULTS

In pH 7.4 at 37°C, the solubility and dose number were found 50.4±4.38 mg/mL and 0.044, respectively (Table 2). The reference and all generic products were dissolved in the range of 78-83% in FeSSIF medium at pH 5.0, 100% in FaSSIF medium at pH 6.5, and 101-103% in pH 7.4, respectively (Figure 2). f_2 values and the suitable mathematical models obtained via DDSolver® are presented in Table 1.

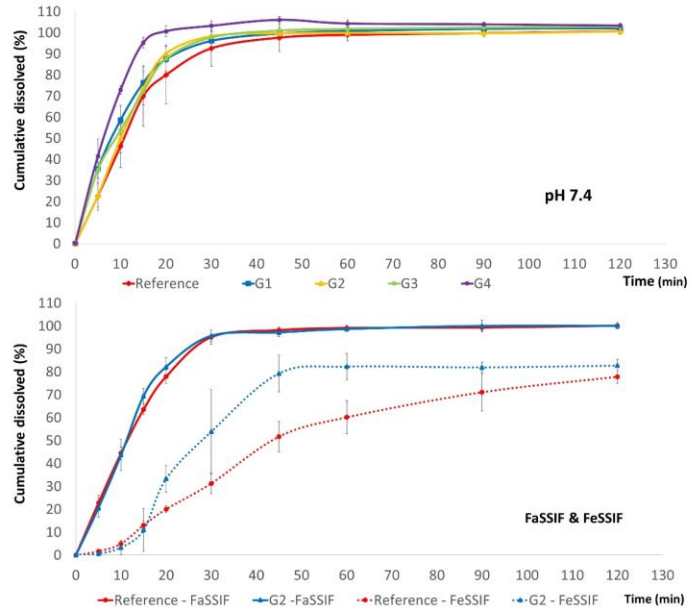

Figure 2. In vitro dissolution profiles of reference and generic products in pH 7.4, FaSSIF, and FeSSIF

Table 2. The solubility, dose number (D_o), and relative sink condition (C_S/C_D) in pH 7.4 at 37°C

Solubility (mg/mL)	D_o	C_S/C_D
50.4±4.38	0.044	82.46

Table 3. Dissolution data analysis of model-independent with DDSolver®

Medium	pH 7.4				FaSSIF	FeSSIF
	G1	G2	G3	G4	G2	G2
f_2	59	69	62	41	79	42
	Similar	Similar	Similar	Different	Similar	Different

Table 4. Dissolution data analysis of model-dependent with DDSolver®

Medium	pH 7.4					FaSSIF		FeSSIF	
	Reference	G1	G2	G3	G4	Reference	G2	Reference	G2
Model	Weibull-1	Weibull-2	Weibull-1	Hopfenberg	Hopfenberg	Hopfenberg	Probit-1	Logistic-2	Logistic-2
r^2 adj	0.997	0.998	0.991	0.996	0.989	0.996	0.994	0.996	0.976
AIC	39.4	31	50.6	40.9	50.8	41.7	46	38	60.5
MSC	4.87	5.42	3.76	4.54	3.33	4.68	4.28	5.03	3.21

CONCLUSION

Biorelevant media were preferred because it mimics in vivo better. NS shows pH-dependent solubility, so as pH increased, solubility increased.

The dissolution profiles of all generic products, except for G4, were found to be similar to the reference product at pH 7.4. Biorelevant media comparison was made for G2 with the highest f_2 and the reference. Model fitting of reference and G2 produced good fits for the same model in each case in pH 7.4 and FeSSIF media.

REFERENCES

[1] Medina, JR et al. (2015). International Journal of Pharmacy and Pharmaceutical Sciences 7, 183-188.
[2] Zhang, Y, et al. (2010). The AAPS Journal 12, 263–271.

ACKNOWLEDGMENT

The authors would like to thank Pharmactive for providing naproxen sodium. **Nebahat Ayşe ERMAN** was supported by a scholarship from The Scientific and Technological Research Council of Turkey (TUBITAK) 2247-C Intern Researcher Scholarship Program (STAR) (Project no: 217S602).

13th International Symposium on Pharmaceutical Sciences (ISOPS), June 22 – 25, 2021

VALIDATED HPLC METHOD FOR THE DETERMINATION OF TENOFOVIR AND ITS APPLICATION FOR IN-VITRO AND EX-VIVO INVESTIGATIONS OF TENOFOVIR LOADED DOUBLE NANOEMULSION

[1]Seval OLGAC, [1]Duygu YILMAZ USTA, [2]Nebahat Ayse ERMAN, [1]Tuba INCECAYIR, [1]Zeynep Safak TEKSIN

[1] Gazi University, Department of Pharmaceutical Technology, Ankara, Turkey

[2] Gazi University, Faculty of Pharmacy, Ankara, Turkey

seval.olgac@gazi.edu.tr

INTRODUCTION

Tenofovir disoproxil fumarate (TDF) is a nucleotide reverse transcriptase inhibitor used for the treatment of hepatitis B and HIV infections [1]. The purpose of this study was to develop a validated HPLC method for the determination of TDF and assess its application for the *in-vitro* and *ex-vivo* studies on TDF formulations.

MATERIALS AND METHODS

Materials

TDF was kindly supplied by Pharmactive drug company (Turkey). Acetonitrile HPLC grade was purchased from Merck. All other chemicals and reagents were of analytical grade.

Methods

The HPLC system (Agilent Technologies 1200 Series) was operated using acetonitrile:ultrapure water (47:53, v/v) as a mobile phase at a flow rate of 1 mL/min. The injection volume was 20 µL. The detection wavelength was 259 nm [2]. Separations were carried out using Waters XSelect HSS C18 column (250x4.6mm, 5µm) at room temperature. The method was validated according to ICH guideline in distilled water and compendial media (0.1N HCl, pH 4.5, and pH 6.8) and has been successfully applied in solubility, dissolution, and permeability studies of TDF formulations [3]. The solubility studies were carried out in distilled water and compendial media. The dissolution of the reference tablet and TDF-loaded double nanoemulsion were studied using USP apparatus II in compendial media. *Ex-vivo* permeability studies of the formulations were carried out using Franz diffusion cells in pH 6.8 buffer for 24h. All collected samples were filtered using a 0.45 µm syringe filter (Sartorius) and analyzed by HPLC. The HPLC method parameters are summarized in Table 1.

Table 1. HPLC method parameters

Column	: RP C18 (4.6 mm x 250 mm, 5 µm)
Mobile Phase	: Acetonitrile : Water (47:53)
Flow Rate	: 1 mL/min
Injection Volume	: 20 µL
Wavelength	: 259 nm, UV-VIS
Column Temperature	: 25°C

RESULTS

HPLC chromatograms of TDF for all media studied are presented in Figure 1. The method was linear in the range of 1-35 µg/mL for all media ($r^2 \geq 0.999$). The retention time of TDF was 3.10-3.96 min in all media. The limit of quantification ranged from 0.394 to 1.140 µg/mL. These parameters are also presented in Table 2. Recovery ranged from 94 to 107%. Within day precision expressed as RSD% were in the range of 0.134 to 1.120. The solubility, dose number (D_o), relative sink condition (C_S/C_D), dissolution, and permeability results are presented in Table 3.

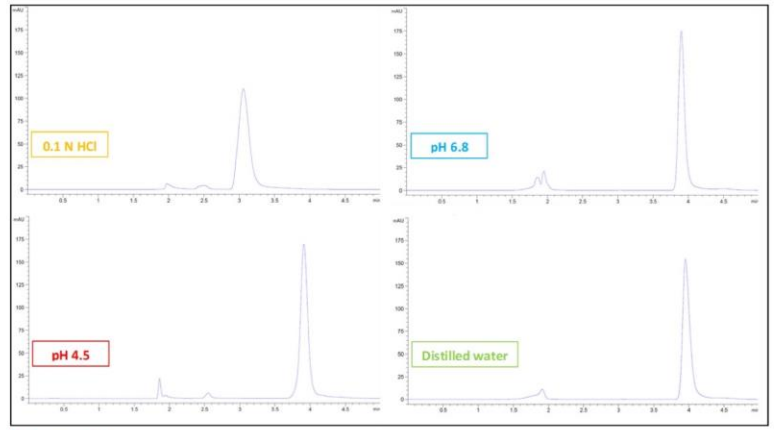

Figure 1. HPLC chromatograms of TDF in all media

Table 2. Validation parameters for all media

	Linear equation	r^2	Retention time*	LOD**	LOQ**
0.1 N HCl	y = 23.519x – 4.5202	0.999	3.10	0.344	1.04
pH 4.5	y = 24.69x – 0.0604	1	3.95	0.130	0.394
pH 6.8	y = 22.923x + 0.7967	0.999	3.90	0.290	0.879
Distilled water	y = 22.591x – 1.5926	0.999	3.96	0.376	1.14

*min, **µg/mL

Table 3. The solubility, D_o, C_S/C_D, dissolution [3] and permeability [3] results

	0.1N HCl	pH 4.5	pH 6.8	Distilled water
Solubility	197 ± 56	30.6 ± 15.8	9.78 ± 0.774	16.4 ± 2.25
D_o	0.00609	0.0392	0.123	0.0731
C_S/C_D	591	91.8	29.3	49.2

Dissolution: 0.1 N HCl		pH 4.5		pH 6.8	
Reference	**Formulation**	**Reference**	**Formulation**	**Reference**	**Formulation**
106 ± 0.754%	98.6 ± 0.935%	97.9 ± 0.813%	91.9 ± 1.53%	95.4 ± 0.783%	88.5 ± 2.82%

	Reference		Formulation	
	Flux*	**Permeability coefficient****	**Flux**	**Permeability coefficient**
Ex-vivo	181 ± 98	90.5±48.9 x 10^{-4}	12.9 ± 6.53	6.47±3.26 x 10^{-4}
Dialysis membrane	758 ± 103	379±52 x 10^{-4}	30.5 ± 15.3	15.2±7.63 x 10^{-4}

* µg.cm^{-2}.min^{-1}, **cm.min^{-1}

CONCLUSION

In conclusion, the HPLC method proved to be sensitive, simple, reproducible, rapid, and precise, making it valuable in the formulation development studies for TDF.

ACKNOWLEDGMENT

Seval OLGAC was supported by a scholarship from The Scientific and Technological Research Council of Turkey (TUBITAK) 2211-C National Ph.D. Scholarship Program in the Priority Fields in Science and Technology. **Nebahat Ayşe ERMAN** was supported by a scholarship from TUBITAK 2247-C Intern Researcher Scholarship Program (STAR) (Project no: 217S602).

REFERENCES

1. Geboers S et al. (2015). International Journal of Pharmaceutics, 485(1-2), 131-137.

2. Kandagal PB et al. (2008). Analytical Letters. 41:4, 561-570.

3. Olgac S et al. (2021). EUFEPS Annual Meeting 2021

JUNE 22-25, 2021 ANKARA, TURKEY

13th International SYMPOSIUM ON PHARMACEUTICAL SCIENCES

JUNE 22-25, 2021
ANKARA, TURKEY

ISOPS 13th International SYMPOSIUM ON PHARMACEUTICAL SCIENCES

ANKARA UNIVERSITY FACULTY OF PHARMACY

INTRANSAL DELIVERY OF NIOSOMAL MELATONIN FOR ALZHEIMER'S DISEASE

Feyza

[1]Görür F. Ş., [1]Uzuner Y, Y.

[1]Acıbadem Mehmet Ali Aydınlar University, Faculty of Pharmacy, Department of Pharmaceutical Technology, İstanbul ,asemin.uzuner@acibadem.edu.tr

ACIBADEM MEHMET ALİ AYDINLAR UNIVERSITY FACULTY OF PHARMACY
REPUBLIC OF TURKEY

Abstract

Melatonin is a methoxyindole hormone which present in vertabrates,synthesized in the pineal gland [1]gut,skin,retina,bone marrow and platelets.It is produces by bacteria,protozoa and fungi as well[2].Its structure,especially its two functional groups are crucial forbinding affinity to certain receptors and also flexibility allowing it to enter any cell,body fluid and compartment to insert its effects [3].Melatonin is gaining popularity due to its many benefits in diabetes, anxiety, cancer, narcolepsy, insomnia, jet lag,anti-aging and neurodegeneretive disorders like dementia, Parkinson's disease and Alzheimer's Disease. Recent studies showed that intra-nasal route offer many advantages, such as presence of large absorption surface area and porous nature of endotelial membrane,high blood flow in the area, avoidance of first-pass metabolism and ease of application. Melatonin delivery into brain as a targeted delivery may offer a good opportunity as a novel delivery system for the treatment of CNS diseases. In this study the aim was to develop and characterize an intra-nasal niosomal melatonin formulation.

Using thin film hydration, hand shaking and ultrasonication method, 3 different batches of niosomes were preapared. Niosomes were characterized by determining their mean particle sizes and particle size distributions, and measuring the zeta potentials and entrapment efficiencies. *In- vitro* release studies were also conducted by using Franzcell Diffusion chambers comparing the release behaviours from niosomes, supernatant solutions and the hydration solutions used in forming niosomes. The samples collected from the diffusion cells were analyzed with LC-MS. The images of niosomes were captured by the transmission electron microscope.

Key words: Melatonin, niosomes; Alzheimers disease, nasal delivery

Introduction

- **Alzheimer's disease (AD)** One of the most costly disease in first World countries.
- 50 million people Worldwide suffer from AD according to 2020 numbers
- Loss of short memory, difficulty in talking, retardation in attention, mood swings, impaired movements are major symptoms
- Death causes are respiratory disorders, pneumonia and pressure ulcers, malnutrition
- Exact mechansim of its patalogy is still not known certainly, but 2 main mechanisms are suggested

1) Amyloid Beta induced neurotoxicity

- Degradation of Amyloid precursor protein results in formation of Aβ oligomer clusters which forms Aβ fibrils and β plaques.
- Oligomeric Aβ binds to receptors in postsynapeses causing LTP impairment and increased LTD,resulting transduction of synaptotoxicity and disturbance in synaptic function.
- Oligomeric Aβ alters the function of mitochondria leading to ATP reduction through caspase-3 activation causing an increase in ROS and finally results in syaptic dysfunction.

2) Tau Pathogenesis

- Seperation of Tau from microtubules and formation of tau oligomers
- Tau clusters cause the fragmentation of mitochondria
- Decreases the mobility and release of synaptic vesicles results in pre-synaptic dysfunction
- Tau species alters Fyn/NMDAR complexes leading to impaired LTP
- Tau species activate inflammation pathways

Pathogenesis models are acceptes 70% genetic particularly due to mutations in PP and presenilin. However many researches Show environmental factors and life style may also change the progression of Alzheimer's Disease. Such as smoking,diet,air pollution and sleep patterns.

- **AD Therapy**

Cholinesterase Inhibitors and NMDA Receptor Blockers are used for symptomatic relief. Anti-psychotic drugs are to improve the violent and aggressive behaviours.

Antoxidant and anti-inflammatory agents are suggested to slow down the progression of. Alzheimer's Disease through reducing lipid peroxidation e.g.curcumin, quercetin, melatonin.

Melatonin (MEL) is a sleep hormone mostly assosiated with anti-aging and sleep.

- It is one of the oldest and well known antioxidants in existence.
- Antioxidant feature of MEL makes it beneficial against many disorder and diseases including the AD.
- Antioxidant feature of MEL suggested to improve the free radical problem and Aβ amyloid pathology.
- Also in many studies MEL shown to inhibit some of the syptoms of AD and reduce the sun downing in AD patients.
- **Melatonin and AD**
- MEL decreases the synthesis and accumulation Aβ *in vivo* and *in vitro*
- Scavanges mitochondrial ROS which plays an imporant role in Aβ amyloid toxicity
- MEL found to be suppress apoptosis by inhbiting the action of caspase-3 and increasing the expression of B cell lymphoma-2 in the brain of Aβ induced animal models.
- **NIOSOMES**
- Niosomes, are younger group of nanocarriers are in shape of vesicles that are self-assembled,
- Fabricated from cholesterol or other amphiphilic molecules nonionic surfactants and/or in required quantities
- Less toxic
- Improved bioavaiblity
- Improved solubility
- Better stability
- **WHY NIOSOMAL MEL**
- Increase the dosage of intra-nasal
- application.
- Prevents rapid degradation of MEL
- in body.
- Increasing the shelf-life of MEL and possibility of Achieving Targeted delivery

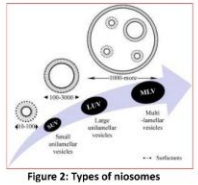

Figure 2: Types of niosomes

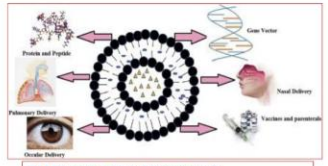

Fig 1 Niosomes as drug delivery systems
Bhardwaj et.al, J DrugDeliv.Sci Tech,(2020),56(A),101518

Methods

- **Characterization of MEL**
  - FT-IR screening
  - TLC to see purity / metabolites
  - Solubility in water and PBS pH 7,4 at 25°C, 37°C
  - Partition coefficient at 25 °C
  - Development of quantitative UV Spectrophotometric method for MEL in water and PBS pH 7,4. ICH Q2(R1) Analytical Method Validation Guidelines was used and all parameters were investigatw

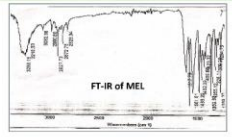

Thin film and Niosome suspension

Figure 4: TEM images of Niosomes

- **Production of MEL niasomes and characterization of them**
  - **Making MEL Niosomes by thin film method**
    - Cholesterol and Span 60 (1:1)was usedto form the niosomes with or without DCP
    - Hydration solution of PBS pH 7,4 contained MEL and varying amounts of MEL was tried to see the effect on entrapment efficiency (EE).
    - Hand shaking was the main dehydration method and ultrasonic bath sonication and ultrasonic probe application were used to reduce the particle size of niosomes

Figure 3: Preparation of niosomes by thin layer

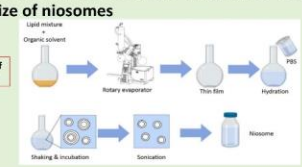

- **Characterisation of MEL niosomes**
- Mean particle size and particle size distribution (PSD) and polidispersity index(PDI). Dynamic Light Scattering (DLS) was used as a method of PS,PSD and PDI
- Zeta potential (ZP) also was used by Anton Paar Zetasizer 500.
- Morphology was investigated and images were photographed by Scanning Electron Microscopy (SEM) on gold grids after several washes by purified water
- Stability at 25°C and at 4-10°C in terms of PSD, PDI and ZP of MEL niosomes were
- Determination of Entrapment Efficiency (% EE) was calculated by using the the equation :
- **MEL Release studies by Franz Cell Diffusion,**
- Niosome suspensions, hydration solution and supernatatnts were used as the donor phase and PBS pH 7.4 was used as the receptor phase
- Released MEL amounts were determined bu LC MS MS

Results:

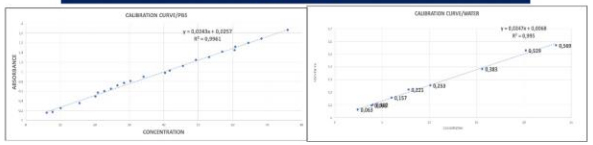

Table 1: Solubility of MEL in water and PBS at 25 °C and 37°C

Solubility of MEL	At 25°C	At 37°C
In water; mg/ml	2,42 ± 0,135	14,03 ± 0,075
In PBS pH 7;4, mg/ml	2,75 ± 0,218	14,03 ± 0,088

Table 2: Particle size and Zeta potential of Niosomes A and C

Niosomes	PS,nm	SD	PDI	SD	ZP, mV	SD
A	375,7	63,55	27,04	3,19	-44,2	1,8
C	648,1	25,56	25,65	13,14	-46,8	2,1
Empty Niosomes	526,4	61,01	26,2	1,53	-63,1	1,0

Table 3: Particle size and Zeta potential of Niosomes remaining in supernatants of the Niosomes A and C

Niosomes in Supernatants	PS,nm	SD	PDI	SD	ZPl, mV	SD
A	149,50	32,57	22,44	4,86	-27,2	1,8
C	163,58	9,84	14,94	7,28	-29	2,1

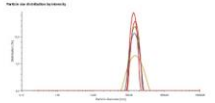

Niosomes (2 hr after sonication)	PS ± SD, nm	PDIe SD	ZP ± SD
X	226,7 ± 12,58	26,7 ± 3,21	-44,7 ± 3,4
Y	226,4 ± 67,71	25,8 ± 3,67	-52,5 ±2,4
Z	176,71 ± 10,09	25,5 ± 2,09	-46,1± 5,6
A-DCP	781,2 ± 11,54	27,2 ± 3,25	-45,2± 1,5
Empty niosomes	166,34 ±9,55	25,4 ± 0,76	-48,5 ± 4,7

Niosomes (24 hr after sonication)	PS ± SD, nm	PDIs SD	ZP ± SD;Mv
X	233,0 ± 26,51	26,5 ± 3,21	-38,1 ± 9,6
Y	249,8 ± 11,78	11,8 ± 3,67	-52,6 ±2,3
Z	206,4 ± 27,69	27,71 ± 2,09	-59,5± 3,2
A-DCP	1281,2 ± 30,85	33,4± 3,25	-45,02± 4,2
Empty niosomes	288,0 ± 37,64	26,5 ± 3,84	-72,5 ± 2,4

Effect of sonication on PS and ZP
Ultrasonic probe was inserted into the tubes and PS and ZP were measured after 2h and 24h.
On the left, the graphs summarizes 2h and 24 h Results, below is the summary of PS distribution curves

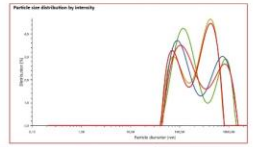

Discussion

- Particle sizes of all batches of niosomes were relatively larger than the desired particles sizes for standard niosomes when just hand shaking and/or sonicator bath is used.
- Probe sonication was a useful and effective method to reduce the particle size and range of particle size distribution.
- DCP was used to increase the surface charges ,ZP, of niosomes, however at the range of DCP used, the effect was negligable.
- When centrifuged, larger sized niosomes could be seperated by forming a pellet, but most of the niosomes remained in the so called supernatant.
- Particle size measurements from the supernatant clearly showed the presence of small particles. These were at the desirable range of the sizes which are suggested in the literature for nasal delivery.
- Up to 6 hours of centrifugation at 10,000 rpm was not able to separate the niosomes, the reasons will be investigated further, by varying the composition of niosomes ; ratio of cholesterol: SPAN 60: DCP: Melatonin
- Higher speed of cenrtrifugation and longer centrifugation time will be tested.
- Zeta potential of the niosomes for all trials were higher than 30 mV, indicating «good to fine « stability.
- Since the seperation of niosomes fully from the supernatant was not possible at the experimental conditions used, %EEs calculated varied widely.
- Bursting the niosomes by adding chloroform released the MEL from the larger sized niosomes.
- The use of smaller sized niosomes, which remained in the supernatant rather than the sedimented niosomes by cetrifugation , may be a good strategy to try it as the drug delivery system.
- Drug release studies showed that niosomes did not release MEL in the length of the time used in the experiments (up to 12 hrs) which is desirable for a good drug delivery system. In-vitro release tests needs to be repeated by allowing the niosomes to come into contact with a larger diffusion area than Franzcell cells, to tests the ability of the niosomes to sustain MEL within them.

Conclusion

- When studying with MEL, much care must be taken in order to assure that it is not degradated. Being an excellent antioxidant, heat and UV exposure degrades MEL fast.
- Possibility of MEL niosomes not readily releasing the drug may make it a good delivery system. Cell culture and *in-vivo* tests are desirable to prove MEL niosomes effectiveness.
- Further formulation studies will be desirable by varying the composition of cholosterol: SPAN 60:MEL, changing the nonionic surfactant and olsa surface charge modifiers to make MEL niosemes as targeted systems.

References

Reiter, R. J., (1993), Experientia, 49(8):654-664.
Liu, C., et al., (2004), Cell Tissue Res, 315(2):197–201.
Stefulj, J., et al., (2001), J Pineal Res.. 30(4):243–247.
Poeggeler, B., et.al. (2002), J. Pineal Res.. 33(1):20–30.
Jing Tang et al.(2015),RSC Advances.30153-30159
Zaheer A., et al (2012) I.J. of Novel Drug Delivery. ; 4(1): 2-16.

Acknowledgement: We would like to Dr. Özgül Gök for her kind assistance in LCMSMS analysis and for valuable discussions.
Our thanks also goes to CRODA Ltd for providing Span 60 .

SYNTHESIS OF CISPLATIN AND/OR GEMCITABINE CONTAINING POLYMERIC NANODRUG FORMULATIONS FOR BREAST CANCER TREATMENT.

[1] Gençoglu, T., [2]Cetin, B., [1]Yigit-Erdem, G., [3]Omurtag-Özgen, PS., [4]Dag, A.

INTRODUCTION AND AIM OF PROJECT

Many anti-cancer drugs have serious side effects, have a short plasma half-life and lack of selectivity. There are treatment methods that directly target cancer cells to overcome these problems. One of the most common method, drug delivery systems are able to reduce side effects and improve efficiency of treament besides targeting anticancer drug to the tumor site [1]. The aim of this study was to prepare a new dual nanodrug formulation based on polymeric drug delivery systems for breast cancer treatment by using Gemcitabine (Gem) and Cisplatin (cisPt) together.

METHODS

Diblock copolymer were synthesize consist of (meth)acrylated sugar monomers and methacrylic acid via RAFT controlled polymerization technique by using Gem functionalized trithiocarbonate RAFT agent. Glycopolymers were analyzed by fourier transform infrared resonance spectroscopy (FTIR) (Figure 1a.) and gel permation chromatıgraphy (GPC) (Figure 1b.). Afterwards the well-characterized glycoblock copolymers conjugated with cisPt to obtain dual drug loaded polymeric nanoparticles. (Figure 2)

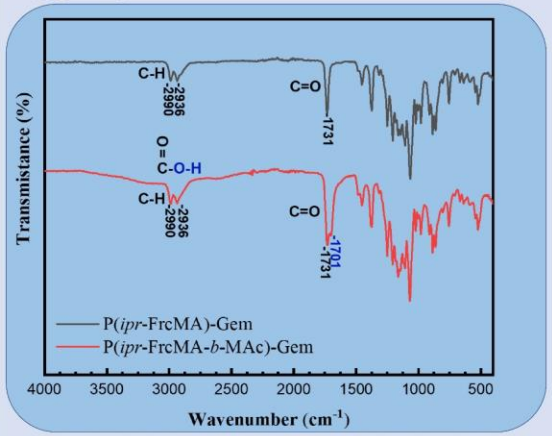

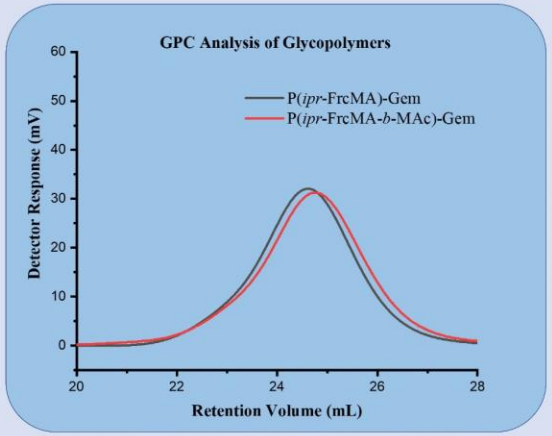

Figure 1. FTIR spectrum (**a**) and GPC graph (**b**) of glycoblock polymers.

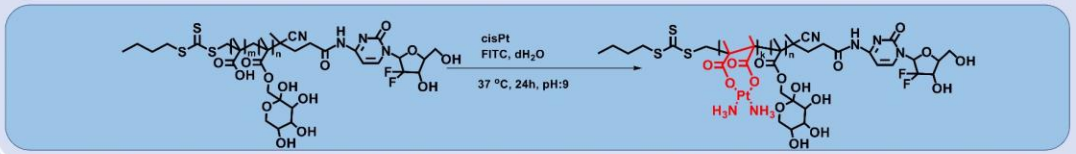

Figure 2. cisPt loading to diblock (FrcMA-*b*-Mac)-Gem glycopolymer in 37 °C for 24 hours at pH 9.

RESULTS:

Size distribution and zeta potential of the nanoparticles were characterized by and dynamic light scattering (DLS) analysis.(Figure 3). According to DLS analysis Gem and cisPt including nanoparticles have average diameter in the 105±3.148 nm range with narrow particle size distribution.

in Vitro cell culture experimentss were performed to determination of cytotoxicity and intracellular uptake of nanoparticle These nanoparticles showed superior uptake and the highest cytotoxicity in-vitro on human breast cancer cells. Figure 4. shows fluorescence microscopy images of NP(FrcMA-*b*-Mac).

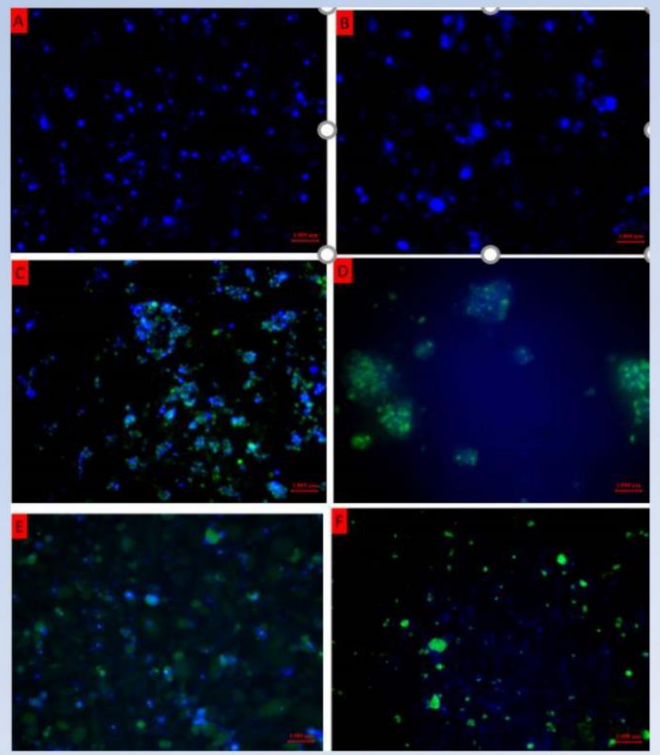

Figure 4. Fluorescent microscopy images of untreated CDD-1079Sk cells(A) and MDA-MB 231 cells (B), Gem and cisPt containing nanoparticle treated at the end of the 3rd hour (C) and 6th hour (D) CDD-1079Sk cells, Gem and cisPt containing nanoparticle treated at the end of 3rd hour(E) and 6th hour (F) MDA-MB 231 cells.

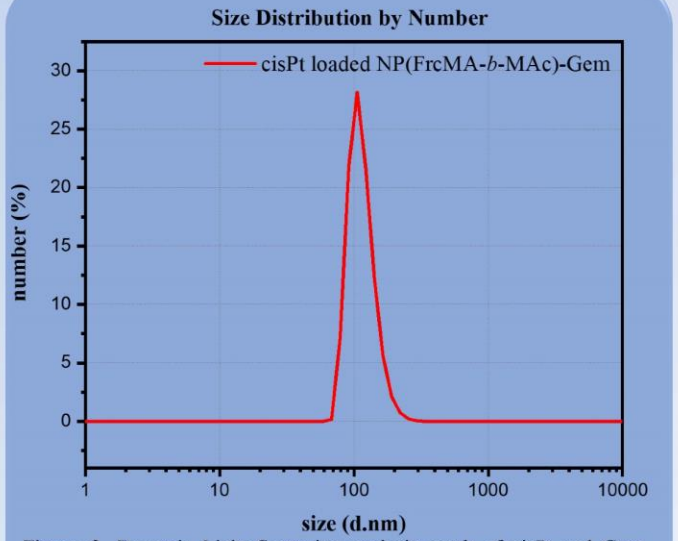

Figure 3. Dynamic Light Scattering analysis result of cisPt and Gem including NP(FrcMA-*b*-Mac).

ACKNOWLEDGMENTS

This project is supported by Bezmialem Vakif University Scientific Research Projects Unit (Project No: 20200919)

[1]Bezmialem Vakif University, Department of Biotechnology, Istanbul, Turkey, ttugbagencoglu@gmail.com, gulsahyigiterdem@gmail.com

[2]Gazi University, Department of Chemistry, Ankara, Turkey, bcbusracetinn@gmail.com

[3]Istanbul Medipol University, Department of Analytical Chemistry, Istanbul, Turkey, psozgen@medipol.edu.tr

[4]Bezmialem Vakif University, Department of Pharmaceutical Chemistry, Istanbul, Turkey, adag@bezmialem.edu.tr

TRANSCRIPTOMIC CHARACTERIZATION OF THE USNIC ACID (UA) EFFECTS ON TRIPLE NEGATIVE BREAST CANCER (TNBC) WITH NEXT GENERATION SEQUENCING TECHNOLOGY

[1] Ümmügülsüm TANMAN ·[2]Mine TÜRKTAŞ ERKEN, [1]Demet Cansaran DUMAN
[1] Ankara University, Biotechnology Institute, Ankara, Turkey, gulsumtanman@icloud.com
[1] Ankara University, Biotechnology Institute, Ankara, Turkey, dcansaran@yahoo.com
[2] Gazi University, Faculty of Science, Biology Departmant, Teknikokullar, Ankara, Turkey, mineturktas@gmail.com

INTRODUCTION

One of the most common breast cancer subtypes diagnosed in women is TNBC breast cancer, and an effective treatment method has not yet been developed. Therefore, alternative medicine resources should be used as new treatment options for TNBC treatment. Potentially, one of the ways to search for new anti-cancer drugs is to test various naturally synthesized compounds. In recent years, interest in natural products has increased as a source of anticancer drugs instead of DNA-damaging cytotoxic agents as cancer treatments. Lichens produce unique chemical agents that have proven effective in in vitro models against a variety of cancers.. The efficacy of only some of these chemical agents against cancer models has been evaluated.. Some studies have shown the anticancer potential of UA; however, its efficacy and associated mechanisms have not yet been fully investigated. In this study, the molecular mechanism of usnic acid on TNBC cancer was investigated by next generation sequencing. With the application of UA, the expression change at the mRNA level in TNBC cells and the intracellular signaling mechanisms that are effective were revealed.

METHOD

1- Reproduction of cell lines

2- Determination of cell-specific IC50 doses with the XCELLigence® RTCA S16 cell analysis system

3- RNA isolation from cells treated with usnic acid at IC50 doses and cells grown under their own conditions for control purposes.

4- Illumina Transcriptome Sequencing

5- Bioinformatics analyzes

RESULTS

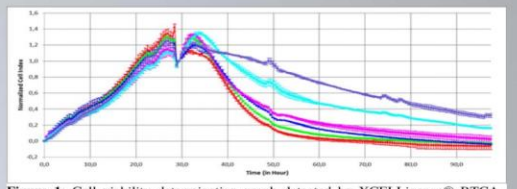

Figure 1: Cell viability determination graph detected by XCELLigence® RTCA S16 measurement in MDA-MB-231 cell line, at determined exponential usnic acid ratios, for 72 hours. In usnic acid ratios, the green curve was represented as 100 µM, the red curve 50 µM, the purple curve 25 µM, the light blue 12.5 µM, the dark blue 6.25 µM, the blue curve 3.125 µM and the pink curve 1.562 µM.

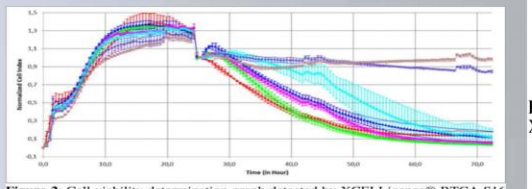

Figure 2: Cell viability determination graph detected by XCELLigence® RTCA S16 measurement in MCF-12A cell line, at determined exponential usnic acid ratios, for 72 hours. In usnic acid ratios, the red curve was represented as 100 µM, green curve 50 µM, purple curve 25 µM, dark blue 12.5 µM, light blue 6.25 µM, blue curve 3.125 µM and pink curve 1.562 µM

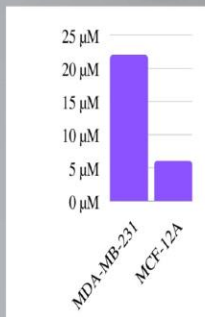

Figure 3: Usnic acid IC50 values calculated using XCELLigence® RTCA S16 instrument

Next Generation Reading Results

Table 1: HiSeq2000 transcriptome reading results for the libraries. (Library names; NM; Healthy/Normal breast cell grown under their own medium conditions. UA_NM; Healthy/Normal epithelial breast cell treated with usnic acid. TNBC; Cancer cell grown under their own medium conditions. UA_TNBC; Cancer cell treated with usnic acid).

Library Name	Total number of bases read	Total number of transcripts read	% GC	% Q20	% Q30
NM	6,084,810,458	40,296,758	50.11	97.61	93.29
UA_NM	5,695,738,724	37,720,124	50.22	97.51	93.12
TNBC	5,333,621,094	35,321,994	50.00	97.41	93.01
UA_TNBC	5,660,695,852	37,488,052	49.24	97.51	93.13

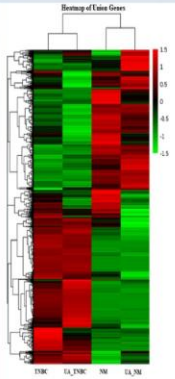

Figure 4: Heatmap of differentially expressed genes (FC > 2 ; Log2 and p<0.005 according to the result of transcriptome analysis (NM: Normal/healthy epithelial brea cell, UA_SM: Normal/healthy epithelial breast cell treated with usnic acid, TNBC Triple negative breast cancer cell, UA_TNBC: Triple negative breast cancer treated wit usnic acid cell; In the color chart, the red color shows increased genes, green color show decreased genes, and black color shows genes that do not show significant expressio changes).

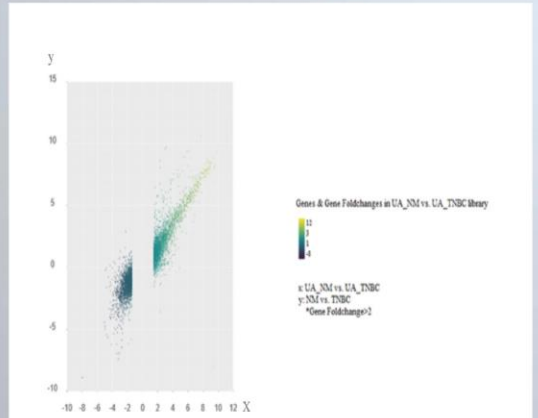

Figure 5: The 4956 genes whose expression changes between usnic acid-treated TNBC cancer and usnic acid-treated normal breast cells are shown in the graph. As a result of the analysis, the coefficient change range of 4956 genes expressed between the UA_NM and UA_TNBC libraries was found to be -8≤FC≤12.

DISCUSSION

- The study showed that usnic acid showed a very different gene expression profile in healthy cells on TNBC cancer.
- Usnic acid acted on TNBC knaser cells by suppressing more genes.
- Usnic acid has also shown an inhibitory function such as suppression of proliferation, metastasis and replicative potential of cells in TNBC cancer cells (1).
- Usnic acid has been integrin, ganodotropin, CCKR, Inflammation, Angiogenesis in TNBC cancer. Usnic acid showed anti-proleferative and anti-metastatic effects in TNBC cancer through these pathways (2,3,4,5)
- The apoptotic effect of usnic acid occurs as a result of degradation in mitochondrial genes (6).

Conclusions: Usnic acid has an anti-tumor effect by suppressing genes that are effective in TNBC cancer formation process

REFERENCES

1- Yang Y, Park SY, Nguyen TT, Yu YH, Nguyen TV, Sun EG, et al. Lichen Secondary Metabolite, Physciosporin, Inhibits Lung Cancer Cell Motility. PLoS One. 2015;10(9):e0137889
2- Aoudjit, F. and K. Vuori, *Integrin signaling in cancer cell survival and chemoresistance.* Chemother Res Pract, 2012. **2012**: p. 283181.
3-Jayaram, S., et al., *Multi-Omics Data Integration and Mapping of Altered Kinases to Pathways Reveal4*
4- Gonadotropin Hormone Signaling in Glioblastoma. OMICS, 2016. **20**(12): p. 736-746..
Jayaram, S., et al., *Multi-Omics Data Integration and Mapping of Altered Kinases to Pathways Reveal Gonadotropin Hormone Signaling in Glioblastoma.* OMICS, 2016. **20**(12): p. 736-746.
5- Rozengurt, E. and J.H. Walsh, *Gastrin, CCK, signaling, and cancer.* Annu Rev Physiol, 2001. **63**: p. 49-76
6- Zuo S-t, Wang L-p, Zhang Y, Zhao D-n, Li Q-s, Shao D, et al. Usnic acid induces apoptosis via an ROS-dependent mitochondrial pathway in human breast cancer cells in vitro and in vivo. RSC Advances. 2015;5(1):153-62.

printed by MegaPrint Inc. www.postersession.com

DETERMINATION THE USNIC ACID (UA) THERAPY EFFECTS ON TRIPLE NEGATIVE BREAST CANCER (TNBC) BY PROTEOMIC APPROACHES

1 Ümmügülsüm TANMAN 1Demet Cansaran DUMAN, 2Mine TÜRKTAŞ ERKEN
1 Ankara University, Biotechnology Institute, Ankara, Turkey, gulsumtanman@icloud.com
1 Ankara University, Biotechnology Institute, Ankara, Turkey, dcansaran@yahoo.com
2 Gazi University, Faculty of Science, Biology Departmant, Teknikokullar, Ankara, Turkey, mineturktas@gmail.com

INTRODUCTION

TNBC cancer is an important clinical problem for which no cure has yet been found. Tends to be more aggressive, associated with worse prognosis than receptor positive subtypes (1). Usnic acid is a lichen secondary metabolite with anti-cancer effects (2). It is extremely valuable to identify proteins that may serve the therapeutic effect of usnic acid on TNBC cancer (3). At the same time, elucidating the therapeutic effect of the new drug candidate molecule usnic acid on TNBC cancer at the proteome level has led to the identification of new therapeutic targets for the treatment of the disease.

METHODS

- Replication of cell lines
- MCF12A for healthy cell and MDA-MB-231 cell line for TNBC cancer were replicated
- Preparation of usnic acid and its application to cells at IC50 doses
- Protein isolations from cells with and without usnic acid treatment
- Protein profiling by LC-MS/MS

RESULTS

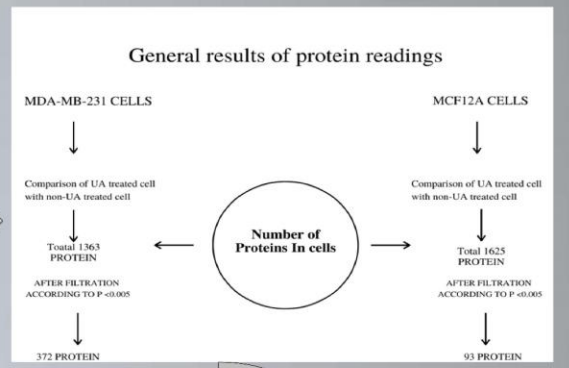

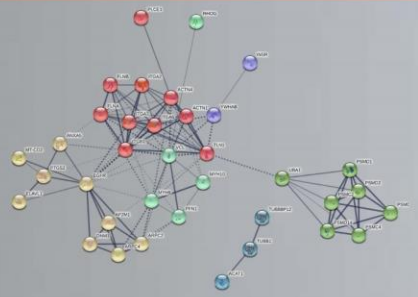

Figure 3: Interaction analysis of the 6 most effective pathway proteins in TNBC cancer. In the bottom inset, one enriched function has been selected, and the corresponding protein nodes in the network are automatically highlighted in color. Pathways represented by each color; Red is integrin pathway, yellow is ganodotropine pathway, blue is inflammation pathway, green is ubiquitin pathway, dark blue is Rho-GTPase pathway, purple is CCKR pathway proteins.

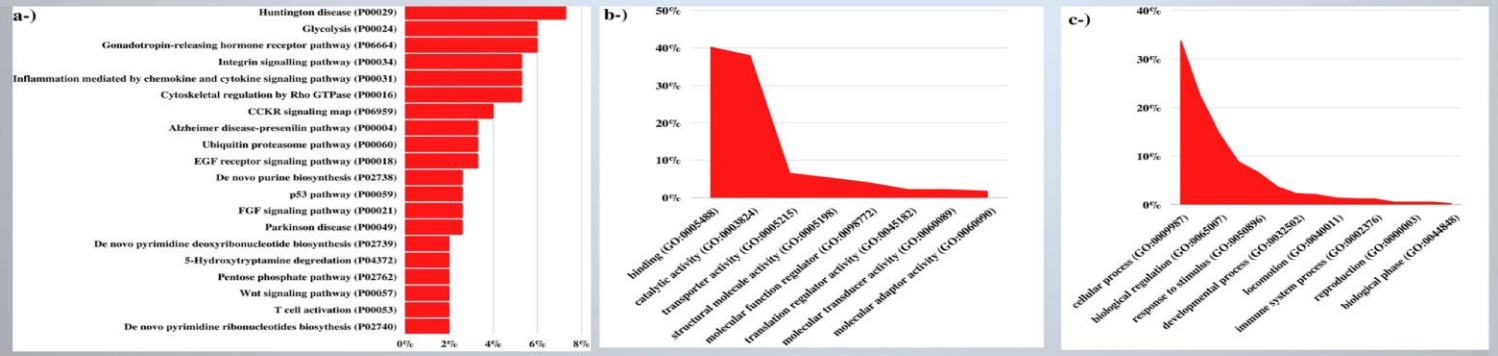

Figure 2: GO and pathway results of usnic acid's proteins (-2≤FC≤2) effective in TNBC cancer (a-; the results of the first 20 pathways in which usnic acid-specific proteins are most effective in TNBC cancer. b-; molecular function results of usnic acid-specific proteins c-; biological process results of usnic acid-specific proteins)

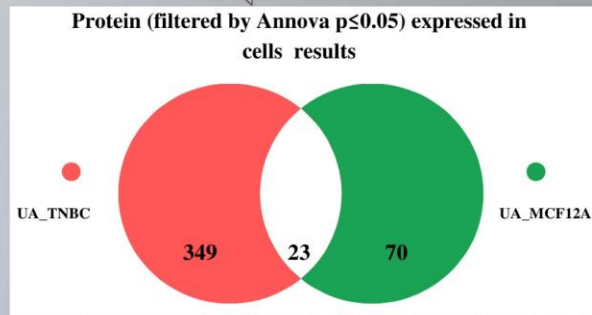

Figure 1: It is the venn diagram representation of the proteins showing the effect of usnic acid on the cells. 70 proteins are proteins that reflect the effect of usnic acid in normal cells. 349 proteins are proteins that show the effect of usnic acid on TNBC cancer. 23 proteins show the joint effect of usnic acid in both cells.

DISCUSSION

- In TNBC cancer, 274 proteins were found with a significant change (-2≤ FC ≤ 2) in UA-specific expression. UA-specific proteins with significant change (-2≤ FC ≤ 2) in TNBC were found to be related to cellular anatomical structure in terms of cellular component, cellular processes in terms of biological process, and binding activities in terms of molecular function
- The most active pathways in TNBC cancer as a result of usnic acid application are Huntington disease, Glycolysis, Gonadotropin pathway, Integrin signaling pathway, Inflammation pathway, CCKR signaling and Ubiquitin proteasome pathway
- Usnic acid treatment regulates extracellular matrix proteins in TNBC cancer.
- Usnic acid creates an apoptotic effect through integrin, inflammation and ubiquitin pathways (4). UA suppresses metastasis and migration with ganodotropin and CCKR pathways (5).

CONCLUSION

UA directs TNBC cells to apoptosis by separating them from the tumor microenvironment using in particularly integrin and ganodotropin pathways.

REFERENCES

1- Judes, G., et al., *High-throughput <<Omics>> technologies: New tools for the study of triple-negative breast cancer.* Cancer Lett, 2016. **382**(1): p. 77-85.
2- Zuo, S.-t., et al., *Usnic acid induces apoptosis via an ROS-dependent mitochondrial pathway in human breast cancer cells in vitro and in vivo.* RSC Advances, 2015. **5**(1): p. 153-162.
3- Lawrence, Robert T., et al., *The Proteomic Landscape of Triple-Negative Breast Cancer.* Cell Reports, 2015. **11**(4): p. 630-644.
4- Jayaram, S., et al., *Multi-Omics Data Integration and Mapping of Altered Kinases to Pathways Reveal Gonadotropin Hormone Signaling in Glioblastoma.* OMICS, 2016. **20**(12): p. 736-746.
5- Rozengurt, E. and J.H. Walsh, *Gastrin, CCK, signaling, and cancer.* Annu Rev Physiol, 2001. **63**: p. 49-76.

printed by MegaPrint Inc. www.postersession.com

BEZMİÂLEM VAKIF ÜNİVERSİTESİ
MEDİPOL UNV-İSTANBUL İSTANBUL MEDİPOL ÜNİVERSİTESİ
JUNE 22-25, 2021 ANKARA, TURKEY
ANKARA UNIVERSITY FACULTY OF PHARMACY
ISOPS 13th International SYMPOSIUM ON PHARMACEUTICAL SCIENCES

INVESTIGATION OF THE EFFECTIVENESS OF GLYCOPOLYMER BASED THERANOSTIC NANOSYSTEMS IN BREAST CANCER

Gülşah YİĞİT ERDEM, Pınar Sinem OMURTAG ÖZGEN, Aydan DAĞ*

Department of Biotechnology, Bezmiale Vakif University, Fatih, Istanbul, Turkey gulsahyigiterdem@gmail.com

Introduction

Nowadays, breast cancer is the most common type of cancer in women in the world. The heterogenecity of cancer cells, stages of cancer, and few similarities make the therapy difficult. Today surgery, chemotherapy, hormonotherapy and radiotherapy methods are applied in treatment of breast cancer. Because of conventional chemotherapeutic agents such as Docetaxel, Doxorubicin (Dox), Epirubicin, have lack of selectivity to tumorous tissue, damage healthy cells, and form serious side effects during treatment, have encouraged scientists to develop new targetable drugs and drug delivery systems.

In recent years, new nanoformulations are being developed that allow targeted imaging, molecular therapy and clinical applications that combine diagnosis and treatment into a single material. This platform, termed as teranostic, allows for the next generation of treatments with the combination of treatments already applied. Because of their low toxicity values, easy to synthesize, modification and application with other imaging technologies, upconversion luminescent nanoparticles (UCNP) is a pioncer in theranostic applications. In addition chemotherapy as well as, photodynamic therapy (PDT) and fototermal therapy (PTT) can be combined with UCNP in therapeutic applications. The aim of this study is to prepare a biocompatible new nanoteranostic platform and to obtain an ideal dual drug/gene delivery system against cancer.

SYNTHESIS and CHARACTERIZATION

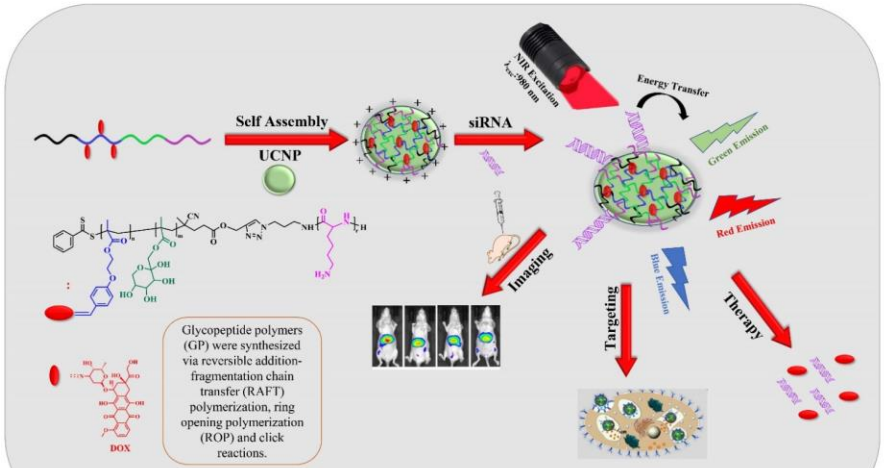

Figure 1. Synthesis and theranostic applications of UCNP@GP-Dox bionanoprobes carrying siRNA.

References:

1. Yan C, Zhao H, Guner S, Perepichka DF, Rosei F (2016). Small, 29: 3888–3907.
2. Dag A, Cakilkaya E, Omurtag Ozgen PS, Atasoy S, Yigit Erdem G, Cetin B, Çavuş Kokuroğlu A, Gürek AG (2021). Biomacromolecules, 22: 1555−1567.
3. Hernandez JR, Klok HA (2003). Journal Of Polymer Science: Part A: Polymer Chemistry, 41, 1167–1187.
4. Li Z, Zhang Y and Jiang S (2008). Adv. Mater., 20, 4765–4769.
5. Qiu X, Zhu X, Su X, Xu M, Yuan W, Liu Q, Xue M, Liu Y, Feng W and Li F (2008). Adv. Sci. 2019, 6, 1801834.

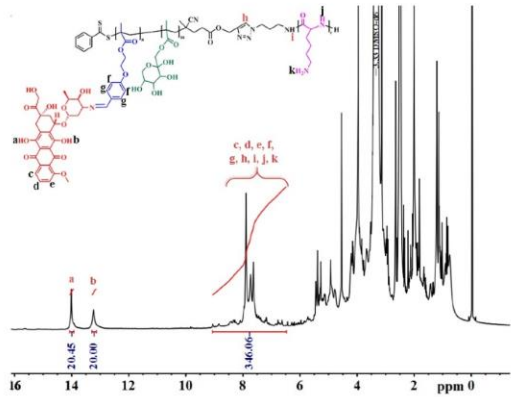

Figure 2. ^{1}H-NMR spectrums of P((FrMA-*b*-MAEBA)-*b*-(P(Lys)-N_3)/Dox in DMSO-d_6.

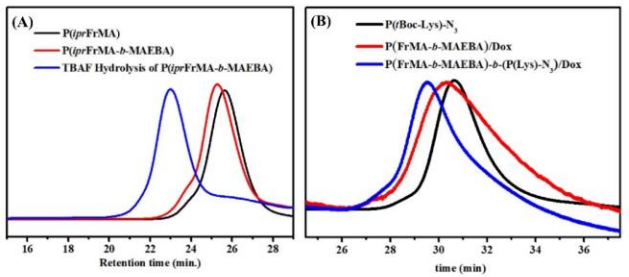

Figure 3. THF-GPC traces of P(*ipr*FrMA), P(*ipr*FrMA-*b*-MAEBA) and TBAF hydrolysis of P(*ipr*FrMA-*b*-MAEBA) **(A)**, DMF-GPC traces of P(*t*Boc-Lys)-N_3 P(FrMA-*b*-MAEBA)/Dox and P((FrMA-*b*-MAEBA)-*b*-(P(Lys)-N_3))/Dox **(B)**.

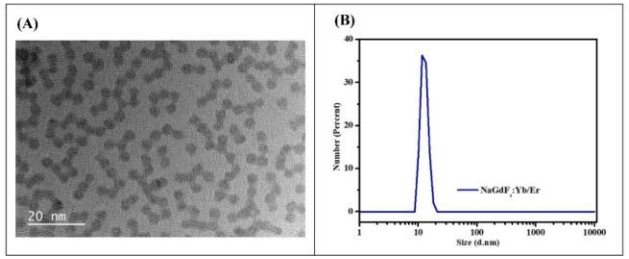

Figure 4. TEM image (left) (A) and Dynamic light scattering (DLS) graph (right) (B) depicting the size of $NaGdF_4$:Yb/Er nanocrystals (UCNP) in cyclohexane.

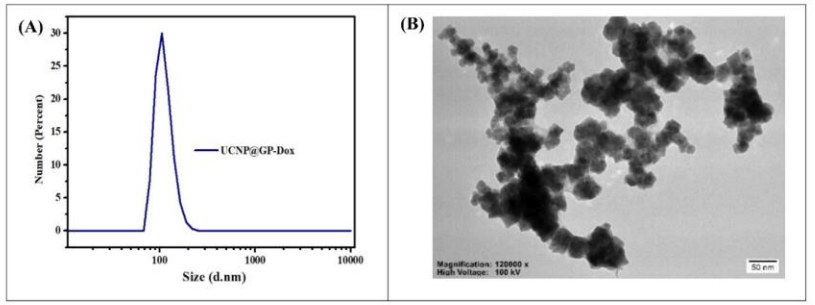

Figure 5. DLS graph (left) (A) and TEM image (right) (B) showing the size of UCNP@GP-Dox nanoparticles (UCNP) in water.

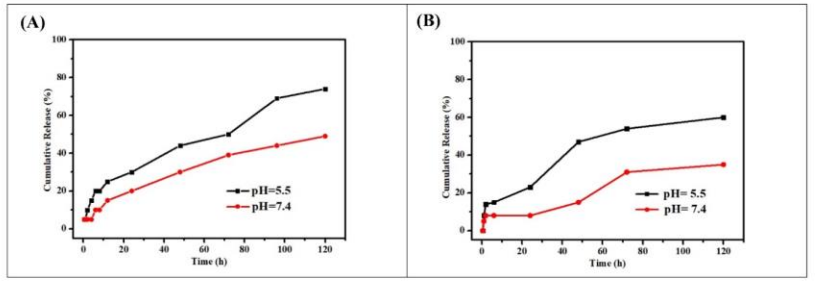

Figure 6. Release of Dox from UCNP@GP-Dox nanoparticles (A) and P((FrMA-*b*-MAEBA)-*b*-(P(Lys)-N_3))/Dox polymer was measured in different pH buffer solutions (pH= 5.5 and pH 7.4) by UV-Vis spectrophotometer.

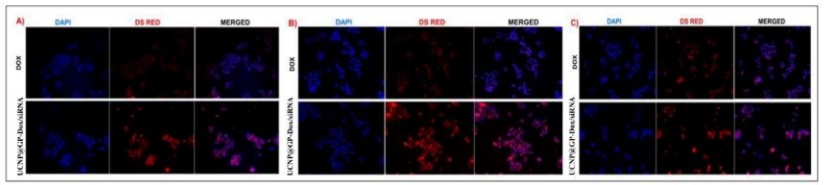

Figure 7. Cellular uptake of free Dox and UCNP@GP-Dox/siRNA by MCF-7 cells after (A) 6 h (B) 12 h (C) 24 h incubation (intracellular Dox shown in red; nuclei shown in blue; and merged images).

Conclusion

In this study, we synthesized well-characterized UCNP@GP-Dox/siRNA. Comparing Dox and UCNP@GP-Dox/siRNA, cellular uptake of UCNP@GP-Dox/siRNA appears to be higher in MCF-7 cell line. In vitro studies showed that UCNPs and GP have low cytotoxicity, siRNA loaded UCNP@GP-Dox have a good cytotoxic and apoptotic effect to human breast cancer cells. The effectiveness of the new nanoteranostic platform in diagnosis and treatment will be demonstrated in future studies.

This study was supported by a grant of TUBITAK (SBAG-118S458) and BAP deparment of Bezmialem Vakif University (Project No: 20210209).

Determination of effective surface modifications of silica nanoparticles as VEGF-targeted siRNA carriers

[1, 2]Ultav, G., [1]Tonbul, H., [2]Salva, E.

[1] Inonu University, Faculty of Pharmacy Department of Pharmaceutical Technology, Malatya, Turkey, gozde.ultav@inonu.edu.tr, hayrettin.tonbul@inonu.edu.tr
[2] Inonu University, Faculty of Pharmacy Department of Biotechnology, Malatya, Turkey, emine.salva@inonu.edu.tr

Introduction: Vascular endothelial growth factor (VEGF) is an endothelial cell-specific mitogen that induces the formation of new capillaries. Tumor cell-derived VEGF-A stimulate angiogenesis and the self-renewal of cancer stem cells [1]. Small interfering RNA (siRNA) targeting VEGF is promising in tumor regression. Due to negative charges, large molecular weight and size, and instability or short half-lives in the plasma, siRNAs can not reach the intracellular target site. In this study, we show that VEGF blocking siRNAs can be carried by PEGylated silica nanoparticles by creation of positive charge on NPs with appropriate surface modifications. The image of designed nanoparticle is given at Figure 1. Particle size, zeta potential, and degree of complexation of nanoparticles were evaluated.

Materials and Methods: All chemicals were purchased from Sigma-Aldrich or Gelest. Silica nanoparticle synthesis method was adopted from Quan et al [2]. 3 experiments were performed as E1 (Surface modification with 3-Triethoxysilylpropylamine (APTES) and PEGylation with Pyridine/ *N*-(3-Dimethylaminopropyl)-*N'*-ethylcarbodiimide (EDC) coupling), E2 (Surface modification with APTES and PEGylation with n-hyroxysuccinimide (NHS)/EDC coupling) and E3 (Surface modification with (3-trimethoxysilylpropyl)diethylenetriamine (TMPT) and PEGylation with PEG-Silane). Particle size determination and zeta potential measurements were done. The agarose gel electrophoresis was performed to evaluate the complexation efficiency.

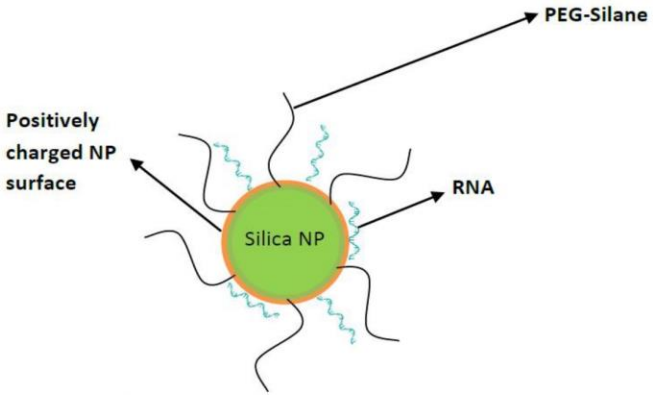

Figure 1. Schematic of the designed nanoparticle

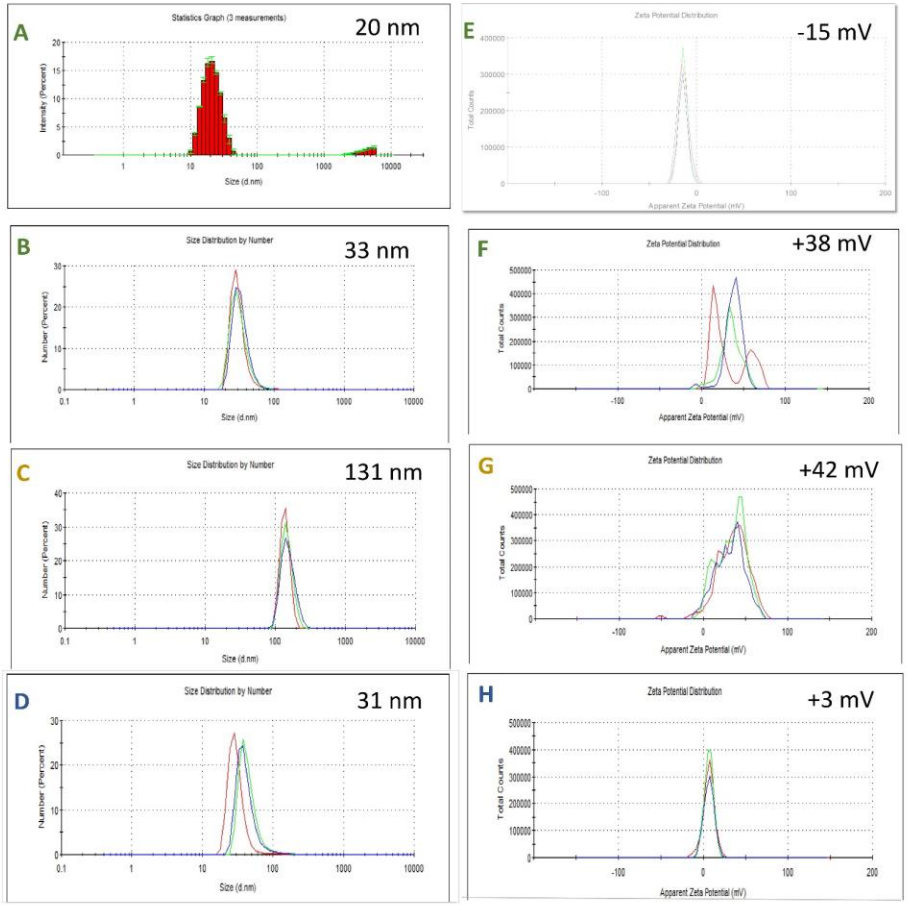

Figure 2. A, B, C and D represents the particles size of the formulations pristine silica, E1, E2 and E3 respectively. E, F, G and H stands for the zeta potentials of the E1, E2 and E3 respectively.

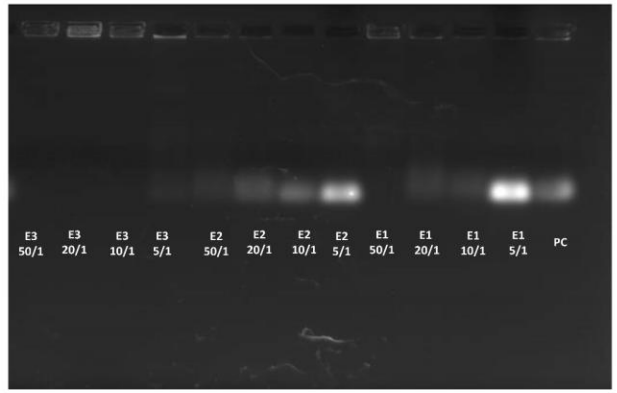

Figure 3. Gel electrophoresis result

Results: Silica NPs were synthesized with the size around 20 nm and zeta potential was -15 mV (Figure 2. A and E). After PEGylation, particle sizes of E1, E2 and E3 were 33 nm, 138 nm and 31 nm, respectively according to Figure 2 B, C and D and all formulations were positively charged according to zeta potential results (Figure 2. F, G and H). These results show that the surface modification was achieved for all 3 formulations and the amine groups were expressed at the nanoparticle surfaces. According the gel electrophoresis results, full complexation was obtained in all ratios of E3 formulation. Complexations were identified for 4 different concentrations as 5/1, 10/1, 20/1 and 50/1 (np/siRNA). After the vortex and incubation for 2 hours, the complexations were determined as below.
E1: full complexation at 50/1
E2: weak complexation at 50/1
E3: Complexation at all ratios.

Conclusions: E3 is the best formulation due to the full complexation with the lower ratios even though the smallest zeta potential. This result shows that the E3 probably deprotonated during the synthesis due to higher pH levels. The surface modification Results show that positively charged and PEGylated silica nanoparticles might be promising approach for siRNA delivery.

Acknowledgements
This study was supported by TUBITAK project 118C470